Final Report

"Smart" Multifunctional Polymers for Enhanced Oil Recovery

For the work performed during the period of

September 2003 through March 2007

by

Charles McCormick

and

Andrew Lowe

Issued on May 5, 2007

DOE Award Number DE-FC26-03NT15407

The University of Southern Mississippi
Department of Polymer Science
Department of Chemistry and Biochemistry
118 College Drive
P.O. Box 10076
Hattiesburg, MS 39406

DISCLAIMER

ABSTRACT

Recent recommendations made by the Department of Energy, in conjunction with ongoing research at the University of Southern Mississippi, have signified a need for the development of *"smart" multi-functional polymers* (SMFPs) for Enhanced Oil Recovery (EOR) processes. Herein we summarize research from the period of September 2003 through March 2007 focusing on both Type I and Type II SMFPs. We have demonstrated the synthesis and behavior of materials that can respond *in situ* to stimuli (ionic strength, pH, temperature, and shear stress). In particular, Type I SMFPs reversibly form micelles in water and have the potential to be utilized in applications that serve to lower interfacial tension at the oil/water interface, resulting in emulsification of oil. Type II SMFPs, which consist of high molecular weight polymers, have been synthesized and have prospective applications related to the modification of fluid viscosity during the recovery process. Through the utilization of these advanced "smart" polymers, the ability to recover more of the original oil in place and a larger portion of that by-passed or deemed "unrecoverable" by conventional chemical flooding should be possible.

TABLE OF CONTENTS

EXECUTIVE SUMMARY

A coordinated, fundamental research program is underway in our laboratories with the *ultimate goal* of developing *"smart" multi-functional polymers* (SMFPs) that can respond *in situ* to stimuli (ionic strength, pH, temperature, and shear stress) resulting in *significantly improved sweep efficiency* in Enhanced Oil Recovery (EOR) processes. With these technologically "smart" polymers, it should be possible to produce more of the original oil in place and a larger portion of that by-passed or deemed "unrecoverable" by conventional chemical flooding. The *specific objectives* of this project are: a) to utilize *recent break-through discoveries* in the Polymer Science Laboratories at the University of Southern Mississippi to tailor polymers with the requisite structures and b) to evaluate the behavioral characteristics and performance of these multifunctional polymers under environmental conditions encountered in the petroleum reservoir. Two structural types of SMFPs are targeted that can work alone or in a concerted fashion in water-flooding processes. Type I SMFPs can reversibly form micelles, termed "polysoaps", in water that serve to lower interfacial tension at the oil/water interface, resulting in emulsification of oil. Type II SMFPs are high molecular weight polymers designed to alter fluid viscosity during the recovery process.

Critical to the desired performance of these conceptual systems is the precise incorporation of selected functional monomers along the macromolecular backbone to serve as *sensors* or *triggers* activated by changes of the surrounding fluid environment. The placement of hydrophilic, hydrophobic, and triggerable monomers is accomplished by controlled free radical polymerization utilizing aqueous Reversible Addition-Fragmentation chain Transfer (RAFT) polymerization, a technique under intensive development in the USM laboratories. The stimuli-responsive functional groups can elicit conformational changes in the polymers which in turn will alter surfactant behavior (Type 1), viscosity (Type II), and permeability to the oil and aqueous phases. Thus, in principle, fluid flow behavior through the porous reservoir rock can be altered by changes in electrolyte concentration, pH, temperature, and flow rate. Significantly, the technology proposed is *environmentally attractive* since these systems can be synthesized in, processed in, separated from or recycled in *water*. Impetus for this study came from priority recommendations made during recent meetings organized by the Department of Energy and from extensive research over the past twenty-five years at USM on Water-Soluble Polymers. An infrastructure providing interdisciplinary research and academic studies in energy and environmental technologies, state-of-the art facilities and instrumentation, student stipends and scholarships, seminars and visiting scientists programs, and international symposia has been developed at USM almost exclusively from funding provided by the Chemical Flooding Program of the Department of Energy and the Environmental (Materials) Program of the Office of Naval Research. We have now trained over 70 students, including 40 PhDs, in fossil energy and environmental technologies. Our current research has the added benefit of continuing the educational training of America's future scientists and engineers and developing frontier EOR technologies critical to America's economic security.

INTRODUCTION
SMFP TYPE II POLYMERS ("Smart" Mobility Control Agents)

Zwitterionic water-soluble polymers have been the subject of extensive investigations in our laboratories due to their unique responsiveness to saline media.[1,2] Unlike polyelectrolytes (PEs), which bear *either* anionic or cationic charges, polyzwitterions (PZs) bear *both* anionic and cationic functionalities.[3-5] PZs are categorized as polyampholytes (anionic and cationic charges on *separate* repeat units) or polybetaines (anionic and cationic charges on the *same* repeat unit).[1,6] Due to their zwitterionic character, PZs exhibit markedly different behavior from PEs in aqueous solution.[4,6-12] In dilute, salt-free aqueous solutions, PEs adopt extended conformations and possess large hydrodynamic volumes due to the electrostatic repulsions of the like charges along the polymer chain;[13] as a result, PE solutions in fresh water tend to maintain high viscosities. However, PEs usually exhibit decreases in hydrodynamic volume and solution viscosity upon the addition of low molecular weight electrolytes (i.e. salts). This PE effect is due to conformational changes that occur when the added electrolytes shield the electrostatic repulsions of like charges along the polymer chain, causing the polymer coils to collapse. Shown below in Figure 1 is a typical plot for PEs of the log of intrinsic viscosity versus the log of salt concentration in which case the polymer conformation is changed from rod-like to coil-like. On the other hand, PZs tend to adopt collapsed or globular conformations in salt-free solutions due to the electrostatic attractions between opposite charges.[9, 11] Indeed, the electrostatic associations are so strong in PZ solutions that the polymers may phase-separate in the absence of low molecular weight electrolytes. However, as simple electrolytes are added to PZ solutions, the electrostatic interactions are shielded, and the PZs can adopt random coil conformations. Sometimes referred to as the "antipolyelectrolyte" effect, the globule-to-coil transition that occurs upon the addition of electrolytes results in increased polymer hydrodynamic volume and solution viscosity, which is exemplified in Figure 2.

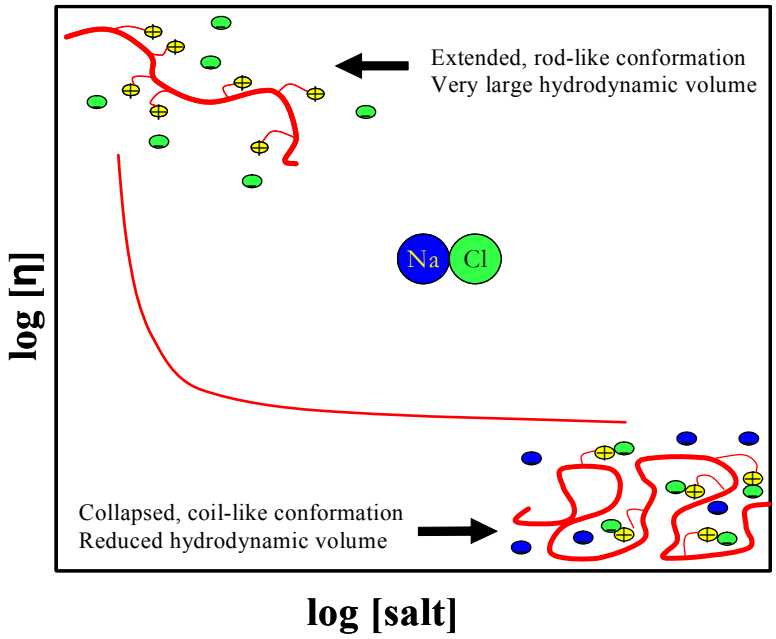

Figure 1. The effect of salt addition on the intrinsic viscosity ([η]) of a polyelectrolyte in aqueous solution.

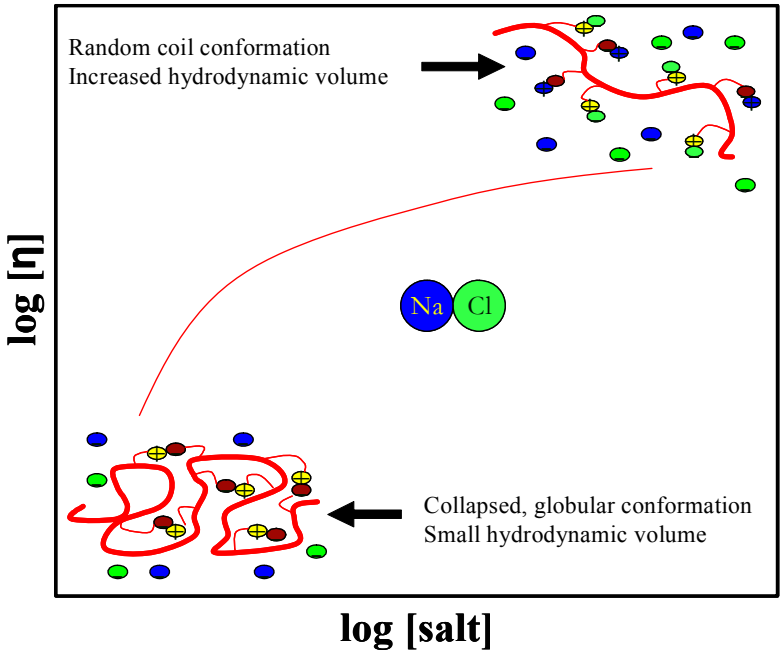

Figure 2. The effect of salt addition on the intrinsic viscosity ([η]) of a polyampholyte in aqueous solution.

Unique salt- responsive behavior is the focus of study in academic laboratories as well as industrial laboratories. Synthetic polyampholytes based on polyacrylamide

(PAM) are excellent prospects for electrolyte-tolerant rheology modifiers, drag reducing agents, and flocculants due to their ability to sustain high solution viscosities in saline conditions as well as exhibit stimuli responsive behavior.[6,14-18] PAM polyampholytes that contain low charge-densities and incorporate large concentrations of acrylamide (AM) are often preferred, due to the fact that long runs of hydrophilic AM repeat units increase the terpolymer solubility at low ionic strengths. The overall performance of low charge-density polyampholyte terpolymers as viscosifying agents is typically greater than that of high charge-density ampholytic copolymers.[14-18] Sulfonate anions and quaternary ammonium cations are the most commonly reported ionic functional groups for most PAM-based polyampholyte systems, and these are known to be insensitive to changes in solution pH.[18-21] Such non-pH-responsive systems are often referred to as *quenched* polyampholytes, and their degree of exhibited polyampholyte or polyelectrolyte character is solely determined by the ratio of anionic-to-cationic monomer incorporation.[18-21] However, when polyampholytes are prepared using comonomers bearing weak acid and/or weak base functionality (e.g. carboxylic acids, tertiary amines, etc.), the degree of polyampholyte or polyelectrolyte behavior exhibited in aqueous solution is governed not only by the ratio of anionic-to-cationic comonomer content, but also by the solution pH.[22-24] Changes in solution pH can elicit either polyampholyte or polyelectrolyte solution behavior, thus allowing the production of functional terpolymers with pH-triggerable solution properties. Such pH-responsive ampholytic systems are referred to as *annealed* polyampholytes.[4] These polyampholytes are well-suited for a range of applications in which pH-triggerable changes in solution viscosity might be useful, for example "smart polymers" for enhanced oil recovery (EOR).

To date, our synthetic research efforts have been focused on the development of stimuli-responsive, water-soluble polymers designed for use in EOR applications.[20, 22-32] These model systems are structurally tailored for potential application as viscosifiers and/or mobility control agents for secondary and tertiary EOR methods. The goal of previous synthetic work has been to design novel polymers that exhibit large dilute solution viscosities in the presence of the adverse conditions normally encountered in oil reservoirs (such as high salt concentrations, the presence of multivalent ions, and elevated temperatures). The polymers are also designed to have "triggerable" properties that can be elicited by external stimuli such as changes in pH and/or salt concentration.

Chemical processes, mainly polymer flooding and surfactant polymer injection, have been the focus of attention of longstanding research in the field of polymer science in relation to EOR. Polymer flooding is based on the principle of improving (decreasing) the mobility difference between injected and in-place reservoir fluids to reduce channeling effects. Mobility control must be maintained within the flood, and the displacing phase should have mobility equal to or lower than the mobility of the oil phase. This mobility ratio, M, is normally expressed:

$$M = \frac{\lambda_w}{\lambda_o} = \frac{\frac{k_w}{\mu_w}}{\frac{k_o}{\mu_o}} \quad (1)$$

λ_w and λ_o represent the mobility of the water and oil respectively while *k* represents permeability to each phase and μ viscosity.[33] When the mobility ratio is one or slightly less, the displacement of the oil by the water phase will occur in a piston-like fashion. By contrast, if the mobility ratio is greater than one, the more mobile water phase will finger through the oil causing "break through" and poor recovery.[34] Based on the principle of the mobility ratio, water soluble polymers can be used to increase the viscosity of the water phase while reducing the permeability of water to the porous rock and thereby creating a more efficient and uniform front to displace oil from the reservoir.[33, 34]

Previous studies in our group have shown that copolymers of AM with low mole fractions of sodium 3-acrylamido-3-methylbutanoate (AMBA) are exceptional viscosifiers compared to conventional anionic PAMs that contain acrylate functionalities.[29] Unlike the hydrolyzed PAMs, these AMBA copolymers are able to maintain viscosity in highly saline media in the presence of divalent cations (e.g. Ca^{2+}, Mg^{2+}) and at elevated temperatures. Under these conditions, solutions of conventional anionic PAMs typically lose viscosity, and precipitation of the polymer may occur.[28, 29]

SMFP TYPE II RESULTS AND DISCUSSION

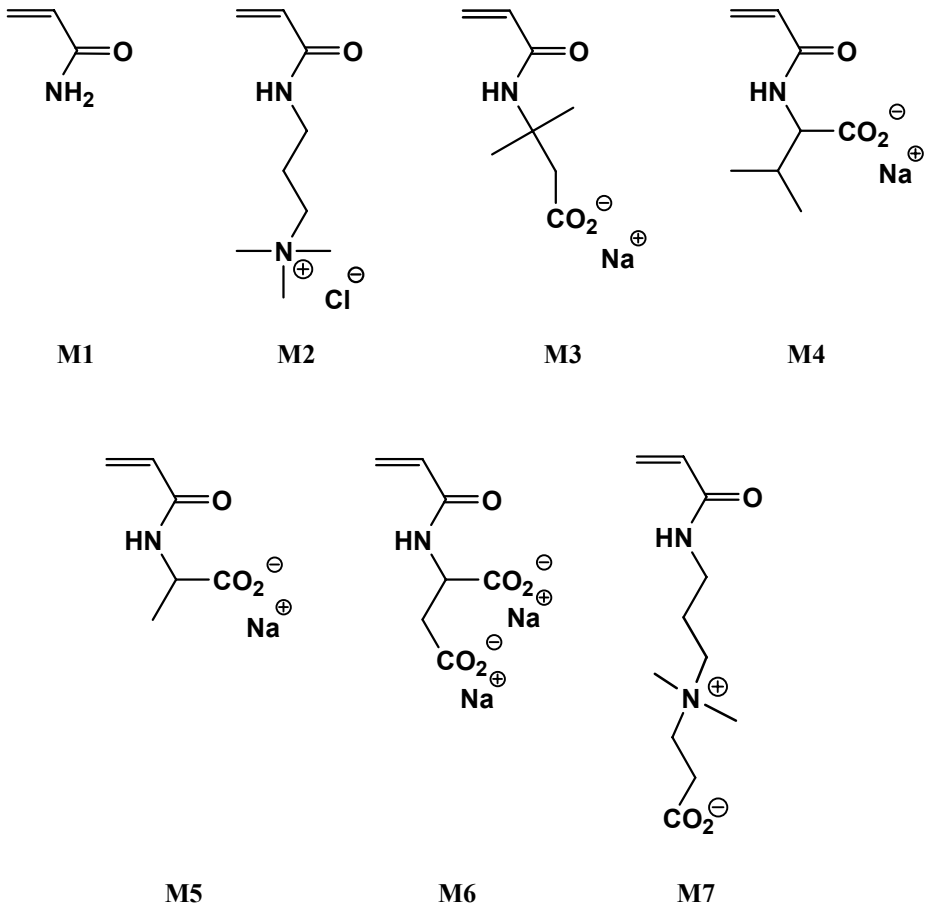

*Figure 3***.** Monomers used to synthesize high molecular weight viscosifiers: acrylamide (AM) (**M1**), (3-acrylamidopropyl)trimethyl ammonium chloride (APTAC) (**M2**), sodium 3-acrylamido-3-methylbutanoate (AMBA) (**M3**), N-acryloyl valine (AVA) (**M4**), N-acryloyl alanine (AAL) (**M5**), and N-acryloyl aspartate (AAS) (**M6**), and 3-(3-acrylamidopropyldimethylammonio)propionate) (AMDAP) (**M7**)

In the study reported here, a comparative analysis of pH-responsive PZs with polyampholyte or polybetaine architectures is conducted utilizing well-defined model polymer systems of similar charge densities. The model PZs include polyampholyte terpolymers of AM (M1), NaAMB (M3), and APTAC (M2), and polybetaine copolymers of AM and 3-(3-acrylamidopropyldiimethylammonio)propionate (APDAP) (M7); the model PZs are referred to as AMBATAC and AMDAP, respectively (Figure 4). The PZs are synthesized via free radical solution polymerization in aqueous media, and the reactions conditions employed have been selected to ensure that the terpolymers possess random charge distributions, are homogeneous in composition, and do not have excessively broad MW distributions (MWDs). The solution properties of model PZs are investigated to elucidate the effects of PZ architecture (i.e. polyampholyte vs. polybetaine) on the stimuli-responsive solution behavior of these systems.

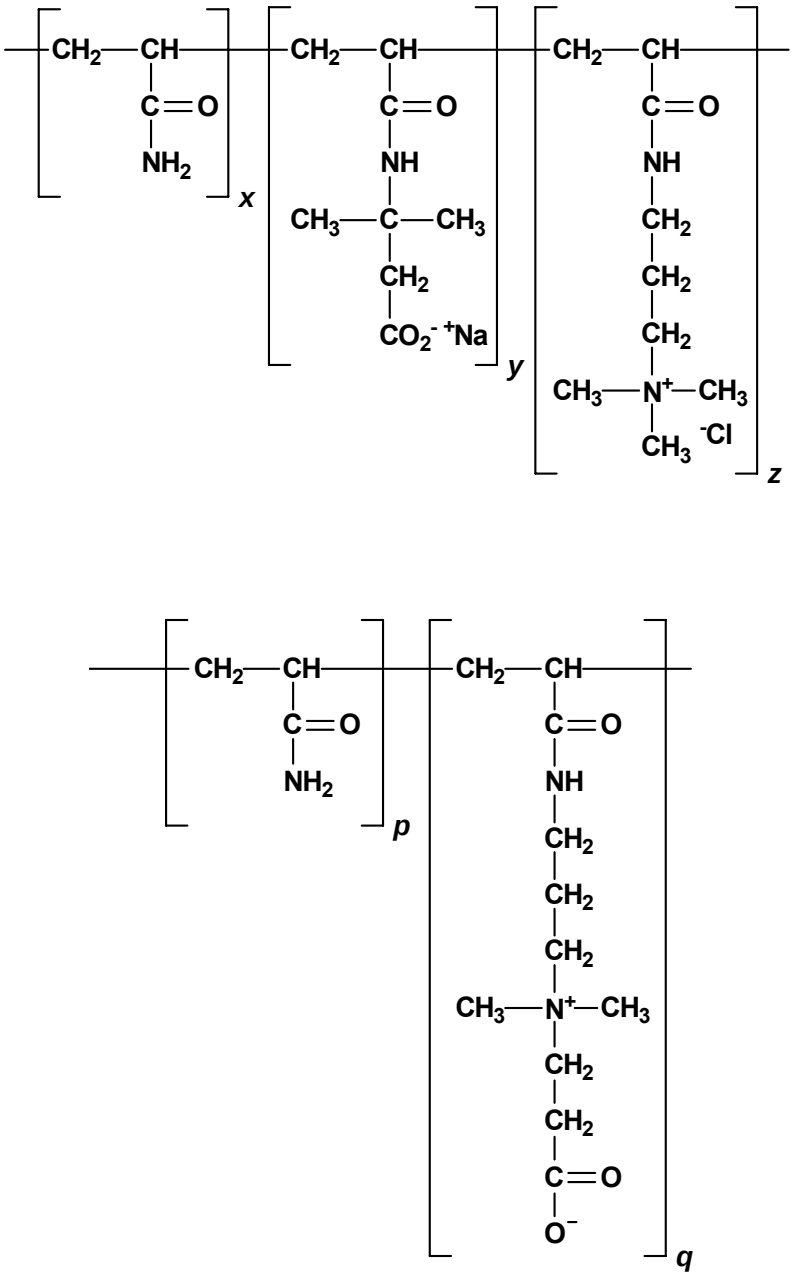

Figure 4. a) Poly(acrylamide-*co*-sodium 3-acrylamido-3-methylbutanoate-*co*-(3-acrylamidopropyl)trimethylammonium chloride) (AMBATAC) polyampholyte terpolymer, and b) poly(acrylamide-*co*-3-(3-acrylamidopropyldimethylammonio)propionate) (AMDAP) polybetaine copolymer.

Table 1. Conversion and compositional data for AMBATAC terpolymer and AMDAP copolymer synthesis.

Sample	Reaction Time (hr)	Conversion[a] (%)	AM[b] (mol %)	NaAMB[b] (mol %)	APTAC[b] (mol %)	APDAP[b] (mol %)
Polyampholytes						
AMBATAC-5-5	6.7	79	91.4	4.6	4.3	-
AMBATAC-10-10	8.0	78	77.9	10.8	11.3	-
Polybetaines						
AMDAP-5	6.8	87	96.0	-	-	4.0
AMDAP-10	6.8	91	90.4	-	-	9.6

[a] conversion determined gravimetrically

[b] determined *via* inverse-gated decoupled ^{13}C NMR spectroscopy

The first column in Table 1 indicates the target compositions of the model PZs synthesized for this study (AMBATAC-*Y*-*Z*, where *Y* = mol % NaAMB and *Z* = mol % APTAC in the monomer feed, and AMDAP-*Q*, where *Q* = mol % APDAP; the balance of both monomer feeds is composed of AM). Charge-balanced AMBATAC terpolymers containing 10–20 mol % total ionic comonomer and APDAP copolymers containing 5–10 mol % zwitterionic comonomer were prepared, corresponding to equal charge densities in the AMBATAC-5-5 and AMDAP-5 and AMBATAC-10-10 and AMDAP-10 systems, respectively. The polymerizations were conducted for six to eight hours to obtain conversions of approximately 80−90 %. It is evident in Table 1 that longer reaction times were required to reach high conversion for the AMBATAC terpolymers. This is attributed to the presence of the hydroquinone monomethyl ether (MEHQ) retarder present in the commercially-available APTAC monomer, which leads to longer induction periods as the level of APTAC in the feed is increased.

Table 2. SEC-MALLS analytical data for AMBATAC terpolymers and AMDAP copolymers.

Sample	d*n*/dc[a] (mL/g)	M_w[b] (10^6 g/mol)	PDI[b]	R_g[b,c] (nm)	$DP \times 10^{-4}$ [d]
Polyampholytes					
AMBATAC-5-5	0.1737	1.51	1.51	65.7	1.90
AMBATAC-10-10	0.1861	1.52	1.65	66.5	1.63
Polybetaines					
AMDAP-5	0.1707	1.43	2.03	61.3	1.85
AMDAP-10	0.1659	1.43	2.11	62.7	1.82

[a] determined in 0.1 M NaCl pH7 phosphate buffer at 25 °C ± 0.5 °C

[b] determined *via* aqueous SEC-MALLS in 0.1 M NaCl pH 7 phosphate buffer

[c] R_g = weight-average radius of gyration

[d] *DP* = weight-average degree of polymerization, calculated from M_w and ^{13}C NMR compositional data

Table 2 lists the values of M_w, PDI, and R_g for the model PZs. The M_w values of the model PZs range from 1.4–1.5 × 10^6 g/mol, corresponding to *DP*s of 1.6–1.9 × 10^4 repeat units. Figure 4 shows the MWDs of the model PZs. The AMBATAC terpolymers exhibit unimodal MWDs of similar shape, with PDI values of 1.51 and 1.65 for AMBATAC-5-5 and -10-10, respectively. The MWDs of the AMDAP-5 and -10 copolymers are slightly broader, with PDIs of 2.03 and 2.11, respectively; nonetheless, the peak values of M_w and *DP* for the model PZs fall in a relatively narrow range. The broader MWDs observed in the AMDAP copolymers are attributed to the higher converions of the AMDAP polymerizations, as PDIs tend to increase with conversion when NaOOCH is used as a chain transfer agent. Overall, these data indicate that the use of NaOOCH in the synthesis of the model PZs is effective at eliminating the effects of monomer feed composition on *DP* and maintaining PDIs ≤ 2.1 by suppressing gel effects. Weight-average values of R_g in the SEC eluent (Table 2) are slightly higher for the AMBATAC terpolymers (66−67 nm) than for the AMDAP terpolymers (61−63 nm), although the polymers are all of similar *DP*s. The values of R_g for the AMBATAC terpolymers are most likely higher due to the lower PDIs of the terpolymer samples.

To fully elucidate the pH- and salt-responsive behavior of the model PZs in dilute solution, the reduced viscosities of AMBATAC terpolymer and AMDAP copolymer solutions (c = 0.1 g/dL) were measured as a function of pH at several values of [NaCl] (Figures 5 and 6). The three-dimensional (3-D) plots shown in Figures 5 and 6 serve as phase diagrams that map the viscosity response to changes in solution pH and salt

concentration. The viscosity response is indicative of the solution behavior (i.e. PZ, PE, or combined PZ-PE) exhibited by the terpolymers at given values of solution pH and [NaCl].

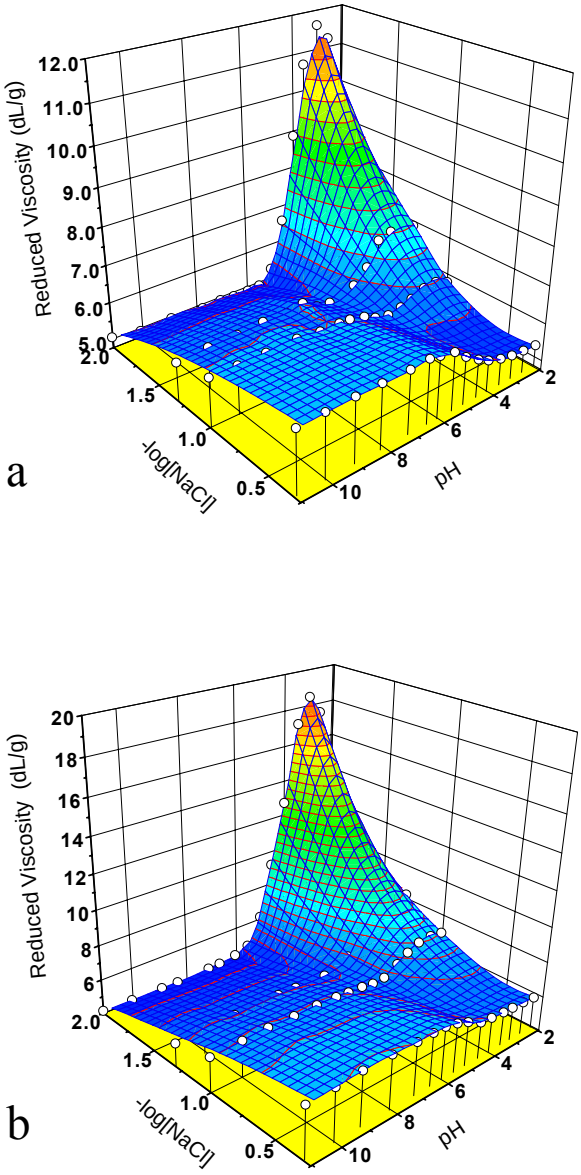

Figure 5. Three-dimensional plots of reduced viscosity as functions of [NaCl] and solution pH for a) AMBATAC-5-5, and b) AMBATAC-10-10. Polymer concentration = 0.1 g/dL. Open circles indicate actual data points.

In Figure 5, four distinct regions are observed in the plots for the AMBATAC-5-5 and -10-10 terpolymers: a) at low [NaCl] and low pH, a PE peak is observed, corresponding to coil expansion due to unscreened electrostatic repulsions; b) at low

[NaCl] and high pH, a polyampholyte valley is observed, indicating coil collapse due to unscreened electrostatic attractions; c) at high [NaCl] and low pH, a PE valley is observed as the electrostatic repulsions are screened at higher ionic strengths and intramolecular hydrogen-bonding predominates, leading to coil collapse; and d) at high [NaCl] and high pH, a polyampholyte plateau is observed, as the increased ionic strength screens electrostatic attractions, allowing coil expansion. Although the contours of the 3-D plots for AMBATAC-5-5 and -10-10 are very similar, it should be noted that the magnitude of the solution viscosity response is significantly greater in AMBATAC-10-10 due to increased charge density.

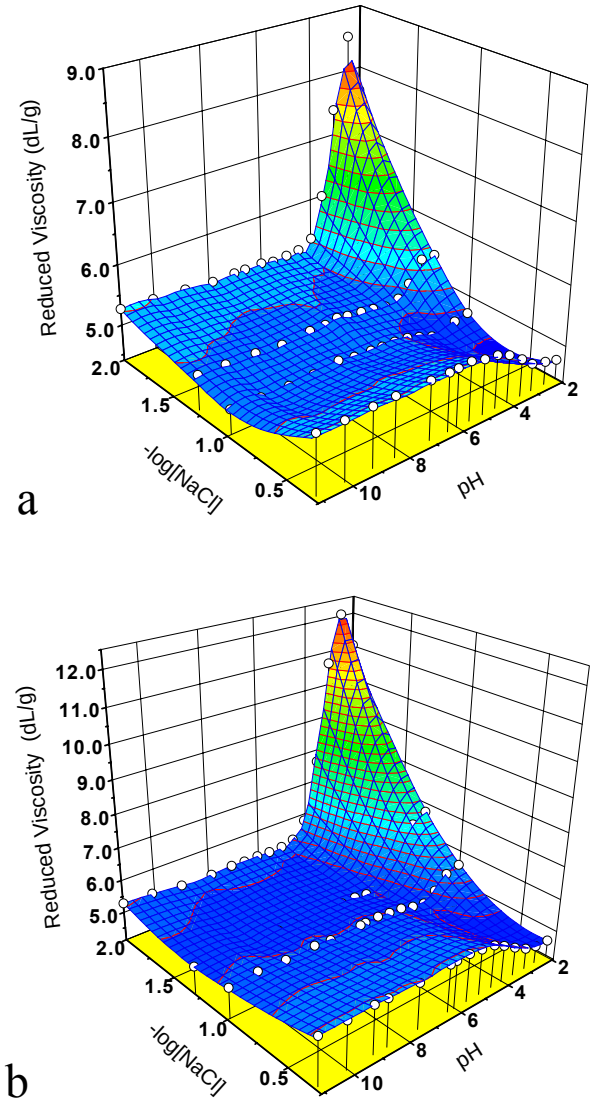

Figure 6. Three-dimensional plots of reduced viscosity as functions of [NaCl] and solution pH for a) AMDAP-5, and b) AMDAP-10. Polymer concentration = 0.1 g/dL. Open circles indicate actual data points.

The 3-D plots for the AMDAP copolymers (Figure 6) reveal less pronounced stimuli-responsive behavior in the polybetaines, as indicated by flatter contour over much of the response space. Nonetheless, the AMDAP copolymers still exhibit the characteristic PE peaks at low [NaCl] and low pH, and PE valleys at high [NaCl] and low pH; however, the PZ response at high ionic strengths is relatively less in the polybetaines, and the AMBATAC terpolymers tend to maintain higher viscosities over wider ranges of solution pH and [NaCl]. For the AMDAP copolymers, the composite effect of weaker dipolar electrostatic interactions and decreased chain stiffness lead to less dramatic changes in polymer conformation and hydrodynamic volume as functions of solution pH and [NaCl], thus the less distinct stimuli-responsive behavior of the polybetaine copolymers.

In summary, SEC-MALLS and viscometric data indicate more open, random coil conformations and greater polymer-solvent interactions in the AMDAP copolymers under SEC conditions. Potentiometric titration studies show that the AMBATAC terpolymers exhibit significantly higher apparent pK_a values than the AMDAP copolymers. The AMBATAC polyampholytes exhibit more pronounced stimuli-responsive solution viscosities and tend to maintain higher solution viscosities over wider ranges of pH and [NaCl]. The differences in solution behavior observed for the AMBATAC polyampholytes and AMDAP polybetaines are attributed to stronger electrostatic interactions and increased chain stiffness in the former.

In another study we examine the effects of structure on dilute solution behavior of terpolymers prepared from acrylamide (AM) (M1), the cationic comonomer (3-acrylamidopropyl)trimethyl ammonium chloride (APTAC) (M2), AMBA (M3) and the amino acid-derived monomers *N*-acryloyl valine (AVA) (M4), *N*-acryloyl alanine (AAL) (M5), and *N*-acryloyl aspartate (AAS) (M6). These amphoteric monomers differ in placement of the carboxylate functionality and spacer group (e.g. the moiety separating the ionic group from the polymer chain) (Figure 1). However, the conformation-dependent intra- and intermolecular associations for respective polyampholyte terpolymers might be expected to be substantially different. The choice of monomers was based on the favorable performance of AMBA in harsh conditions, and the fact that these amino-acid derivatives can be synthesized in a facile, cost-efficient manner from readily available, naturally occurring starting materials. The terpolymers have been synthesized with the goal of creating a well-characterized series of model high MW, low charge density polyampholytes for examination of their stimuli-responsive solution behavior.

Table 3. Properties of the amphoteric polyampholyte terpolymers.

Entry	Polymer[a]	AM (mol %)[b]	Anionic Monomer (mol %)[b]	APTAC (mol %)[b]	M_w (10^6 g/mol)[c]	PDI[c]	h_d[d] (nm)
1C	AM_{90}-AVA_5-TAC_5	90.7	5.0	4.3	1.5	1.52	43.1
2C	AM_{90}-AAL_5-TAC_5	90.2	5.1	4.7	1.1	1.59	43.8
3C	$AM_{92.5}$-$AAS_{2.5}$-TAC_5	92.7	2.7	4.6	1.1	1.40	38.9
4C	AM_{90}-AMB_5-TAC_5	91.4	4.6	4.3	1.5	1.51	43.9

[a] numeric subscripts refer to the mol % of monomer in the reaction medium
[b] determined *via* inverse-gated decoupled ^{13}C NMR and ^{1}H NMR spectroscopy
[c] polydispersity index determined *via* aqueous SEC-MALLS in 0.1 M NaCl pH 7 phosphate buffer
[d] hydrodynamic diameter determined *via* aqueous DLS in 0.1 M NaCl pH 7 phosphate buffer

The first column of Table 3 lists the amphoteric terpolymers synthesized for this study. **1C**-**3C** are the nearly charge-balanced polyampholytes containing the amino acid derived monomers AVA (M4), AAL (M5), and AAS (M6); **4C** is the nearly charge-balanced polyampholyte containing the AMBA monomer. The terpolymers were synthesized with 5.0 mol % of each anionic monomer and 5.0 mol % of APTAC in the feed. Since there are two carboxy groups on the AAS repeating units, the charge density is twice that of the mol % monomer incorporation; therefore, the mol % monomer incorporation is different for **3C** compared to its counterparts in Table 1. Polymerizations were allowed to proceed for 6-7.5 h to obtain conversions of ~ 75%.

As a means of observing the combined pH- and salt-responsive behavior of the polyampholyte terpolymer series in dilute solution, the reduced viscosities of the polyampholyte terpolymer solutions (c = 0.1 g/dL) were measured as functions of pH and [NaCl]. Figure 7 represents three-dimensional (3-D) plots of the combined pH- and salt-responsive characteristics of the polyampholyte terpolymers. These serve as phase diagrams that map the viscosity response to variations in solution pH and salt concentration. Such diagrams are of great practical value in tailoring terpolymer structure for optimal behavior in oil recovery operations; for example, structure can be targeted for a specific viscosity for mobility control in enhanced oil recovery utilizing known values of reservoir salinity and pH.

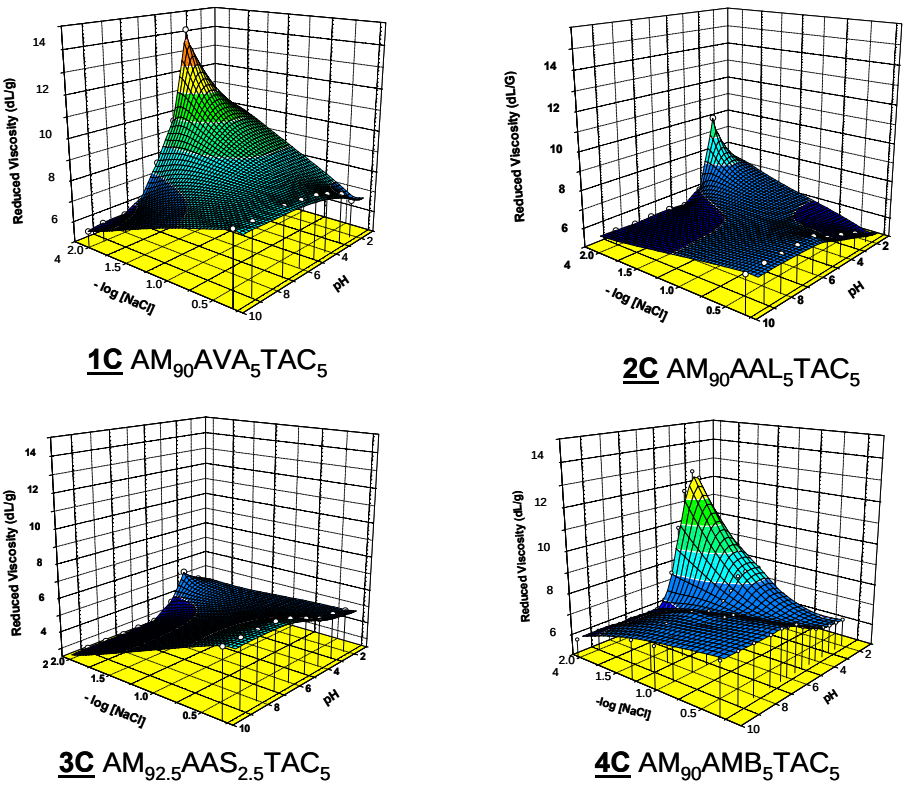

Figure 7. 3D plots of reduced viscosity as functions of the [NaCl] and solution pH for terpolymers 1C – 4C at a concentration of 0.1 g/dL.

In Figure 7, four distinct regions are observed in three dimensional viscosity/[NaCl]/pH plots for each of the stoichiometrically-balanced terpolymers **1C** – **4C**: a) At pH values < 4 and low [NaCl], a maximum is observed, corresponding to coil expansion due to unscreened electrostatic repulsions of uncompensated cationic charges; b) at high pH and low [NaCl], a polyampholyte valley is observed, indicating coil collapse due to unscreened electrostatic attractions; c) at low pH and high [NaCl], a polyelectrolyte valley is observed as the electrostatic repulsions among cationic groups are screened at higher ionic strengths, leading to coil contraction; and d) at high pH and high [NaCl], a polyampholyte plateau is observed, as the increased ionic strength screens electrostatic attractions between cation/anion complexes, allowing coil expansion. Although the contours of the 3-D plots for **1C**-**4C** are very similar, there exist differences in the magnitudes of the solution viscosity responses. We attribute differences to the effects of terpolymer microstructures that result in increased chain stiffness due hydrogen bonding ability of the AVA and AMBA repeat units that limit conformational mobility of **1C** and **4C** while in aqueous solution.

Each particular terpolymer offers advantages in applications such as EOR. For example, the more conformationally-responsive **2C** and **3C** at their isoelectric points can elicit low solution viscosities in DI water which should aid in their injection into porous media with less shear degradation due to low hydrodynamic volumes. Once in the well,

the screening of the electrostatic interactions by in-situ electrolyte would result in globule to coil transitions that cause subsequent increases in solution viscosity and increased mobility control in secondary and tertiary EOR processes. However, terpolymers **1C** and **4C** display more restricted chain conformations in DI water, larger hydrodynamic volumes, and greater solution viscosities. Such behavior is less advantageous to the injection process, but once in the porous media of the well, the viscosity of the terpolymer solutions at/above the isoelectric point is higher than that of **2C** or **3C**. This would result in better control of the waterflood process for EOR.

INTRODUCTION
SMFP TYPE I POLYMERS ("Smart" Polymeric Surfactants)

Water soluble block copolymers capable of undergoing a conformational change or phase transition upon the application of an external stimulus, such as a change in solution pH, electrolyte concentration, or temperature have stimulated a great deal of interest because of their "smart" behavior.[35-42] These materials typically contain both a permanently hydrophilic block as well as a "smart" block which is tunably hydrophilic/hydrophobic. Traditionally, these materials have been prepared using living polymerization methods including anionic, cationic, and group transfer polymerization.[43,44] These techniques, however often require stringent reaction conditions and are restricted to a limited number of relatively non-functional monomers.

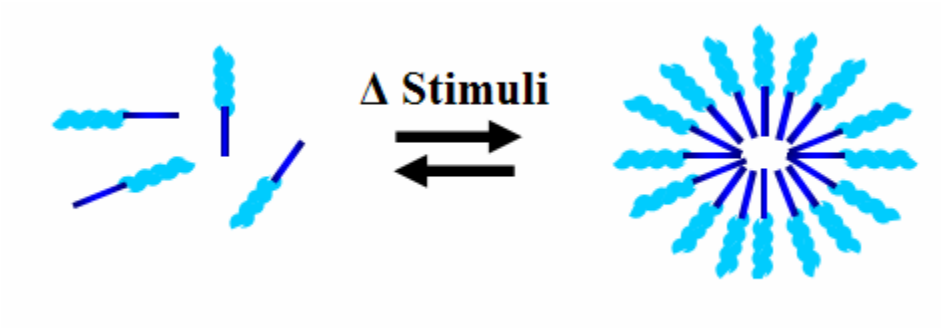

*Scheme 1***.** Self assembly of Stimuli Responsive Polymers

The advancement of several controlled radical polymerization (CRP) techniques has been spurred by the desire to prepare complex architectures (*e.g.* blocks, combs, and stars) with predetermined molecular weights and low polydispersities, while maintaining the robust reaction conditions and wide monomer selection available to radical polymerization. These CRP techniques include nitroxide mediated polymerization (NMP),[45] atom transfer radical polymerization (ATRP),[46] and reversible addition-fragmentation chain transfer (RAFT) polymerization.[47] First introduced by Rizzardo and Moad in 1998, RAFT is arguably the most versatile living radical polymerization technique in terms of monomer selection and reaction conditions.[48,49] The polymerization can be performed in a variety of solvents, including dimethyl formamide and water,

simply by adding the appropriate quantity of a suitable RAFT agent to a standard free radical polymerization.

The direct synthesis of functional block copolymers in aqueous media under mild conditions without protection/deprotection chemistry is a major goal in developing stimuli-responsive delivery systems such as micelles and vesicles. Major advances toward this goal have been realized in RAFT polymerization yielding water-soluble polymers with well-controlled structures. For example homopolymers and block copolymers with anionic,[41, 50] cationic,[51] zwitterionic, [52, 53] and neutral[54-56] functionality have been synthesized directly in water without post-reaction chemistry.

The McCormick Research Group has successfully prepared several stimuli responsive block copolymers that are capable of self assembling into Type I SMFP. This was accomplished through the development of novel chain transfer agents (CTAs) that were essential in controlling the polymerization of monomers utilized in this study. Once this was accomplished, stimuli-responsive block copolymers were synthesized and their aqueous self-assembly properties were investigated. In the subsequent paragraphs the major accomplishments of this work will be highlighted.

SMFP TYPE I RESULTS AND DISCUSSION

The CTAs, monomers, and initiators utilized in this work are presented in Figure 8, Figure 9, and Figure 10, respectively. The complete details for the synthesis and self assembly behavior of the stimuli-responsive block copolymers for DOE Award Number DE-FC26-03NT15407 have been previously reported in quarterly reports beginning April 1, 2004 and ending June 30, 2006. The goal of this report is to highlight the major accomplishments of this work in 5 sections. Specifically, the controlled RAFT polymerization of acrylamide, the synthesis and stimuli responsive behavior of block copolymers of sodium 2-acrylamido-2-methylpropanesulfonate (AMPS) and sodium 3-acrylamido-3methylbutanoate (AMBA), the synthesis and self assembly of diblock copolymers containing a *N*,*N*-dimethylacrylamide (DMA) and *N*,*N*-dimethylvinylbenzylamine (DMVBA), the synthesis and self assembly of block copolymers containing *N*,*N*-dimethylacrylamide (DMA) and *3*-[2-(N-methylacrylamido)-ethyldimethylammonio] propane sulfonate (MAEDAPS), and the synthesis and self assembly of *N*,*N*-dimethylacrylamide (DMA) and *N*-isopropylacrylamide will be highlighted.

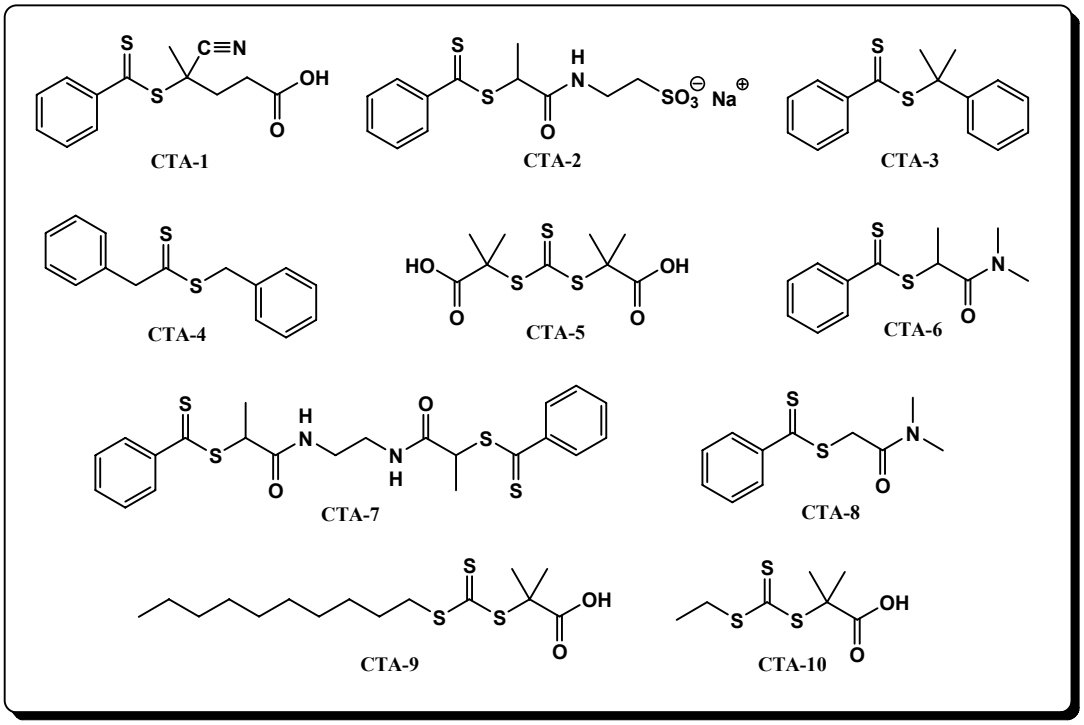

Figure 8. Chain Transfer Agents (CTAs) used for SMFP Type I Synthesis: 4-cyanopentanoic acid dithobenzoate (**CTA-1**), sodium 2-(2-thiobenzoyl sulfonyl-propionylamino)-ethanesulfonate (**CTA-2**), dithiobenzoate (**CTA-3**), cumyl-phenyldithioacetate (**CTA-4**), 2-(1-carboxy-1-methyl-ethylsulfanylthiocarbonylsulfanyl)-2-methylpropionic acid (**CTA-5**), N,N-dimethyl-s-thiobenzoyl-thiopropionamide (**CTA-6**), N,N'-ethylenebis(2-(thiobenzoylthio)propanamide) (**CTA-7**), N,N-dimethyl-s-thiobenzoylthiopropionamide (**CTA-8**), S-dodecyl-S'-(α,α'-dimethyl-α"-acetic acid)trithiocarbonate (**CTA-9**), and S-ethyl-S'-(α,α'-dimethyl-α"-acetic acid)trithiocarbonate

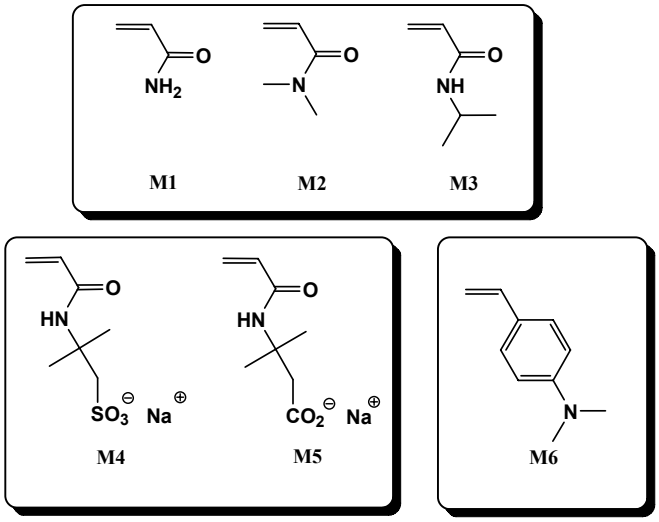

*Figure 9***.** Monomers used for SMFP Type I: acrylamide (AM) (**M1**), N,N-dimethylacrylamide (DMA) (**M2**), N-isopropylacrylamide (NIPAM) (**M3**), sodium 2-acrylamido-2-methylpropanesulfonate (AMPS) (**M4**), sodium 3-acrylamido-3-methylbutanoate (AMBA) (**M5**), and N,N-dimethylvinylbenzylamine (DMVBA) (**M6**)

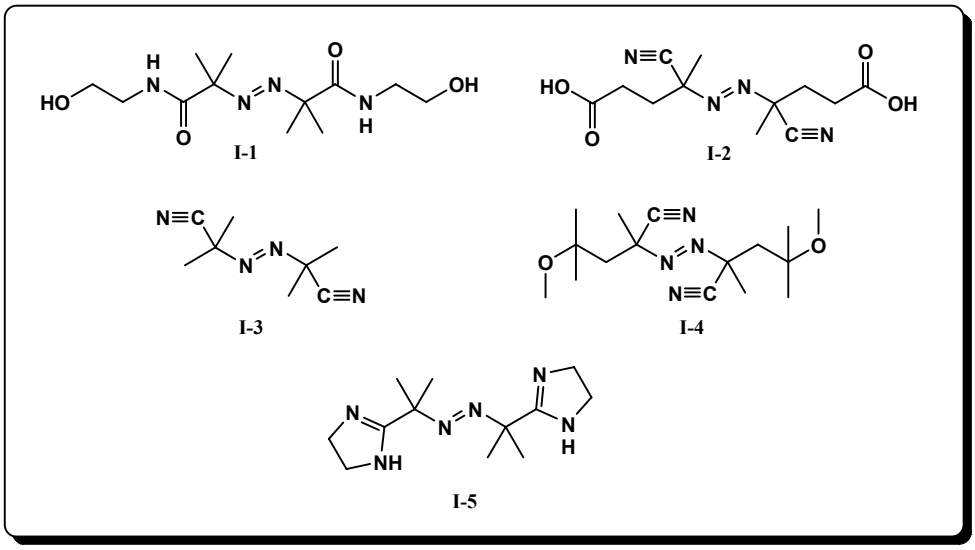

*Figure 10***.** Initiators used for SMFP Type I Synthesis: 2,2'-azobis[N-(2-methyl-N-(2-hydroxyethyl)-propionamide] (VA-086) (**I-1**), 4,4'-azobis(4-cyanovaleric acid) (V-501) (**I-2**), 2,2'-azobis(2-methylpropionitrile) (AIBN) (**I-3**), 2,2'-azobis(4-methoxy-2,4-dimethylvaleronitrile) (V-70) (**I-4**), and 2,2'-azobis[2-(2-imidazolin-2-yl)propane] dihydrochlorine (VA-044) (**I-5**)

Section I.

Acrylamide and DMA are important monomers in the preparation of polymers and copolymers for EOR. Here we demonstrate the ability of RAFT to control the

polymerization of acrylamide (**M1**) directly in water. With all aqueous RAFT polymerizations, the proper selection of reaction conditions (CTA, temperature, pH, etc.) is important in order to achieve ideal results. Most aqueous RAFT polymerizations have been performed utilizing cyanopentanoic acid dithiobenzoate (**CTA-1**) as the CTA. However, this chain transfer agent utilizes a carboxylate functionality to achieve solubility in water. The weakly acidic nature of this group ($pK_a \sim 5.5$) limits the solubility of **CTA-1** under acidic conditions. Accordingly, a new chain transfer agent, sodium 2-(2-thiobenzoylsulfonyl-propionylamino)-ethanesulfonate (STPE) (**CTA-2**), was prepared to allow polymerization under acidic conditions.

After **CTA-2** was prepared, it was utilized in the polymerization of acrylamide at selected solution pH values. Under neutral pH conditions, acrylamide was found to polymerize in an uncontrolled fashion. Under acidic conditions, however, control was achieved and the homopolymer could be used as a macroCTA allowing successful chain extension.

It was found that the polymerization process was best controlled by performing the polymerization (Scheme 2) in an acetic acid/sodium acetate buffer (pH = 5.0). Under these conditions, the pseudo-first order rate plot and the plot of DP_n vs conversion were both linear and thus indicate controlled/"living" polymerization. Polydispersities were generally low (Table 4) ranging from 1.04 to 1.06 at intermediate reaction times.

Table 4. Kinetic and Molecular weight data for the RAFT polymerization of acrylamide in an acetic acid/sodium acetate buffer (pH = 5.0) using **CTA-2** as the CTA.

Polymerization Time (h)	% Conversion[a]	M_n (g/mol)[a]	M_n, theoretical (g/mol)[b]	PDI[a]
0	0	-	-	-
2	3	5 300	1 710	1.15
4	9	9 790	5 120	1.05
8	11	13 700	6 260	1.04
12	18	18 600	10 200	1.06
24	28	28 900	15 900	1.26

[a] determined by ASEC/MALLS
[b] calculated from conversion using Equation 19

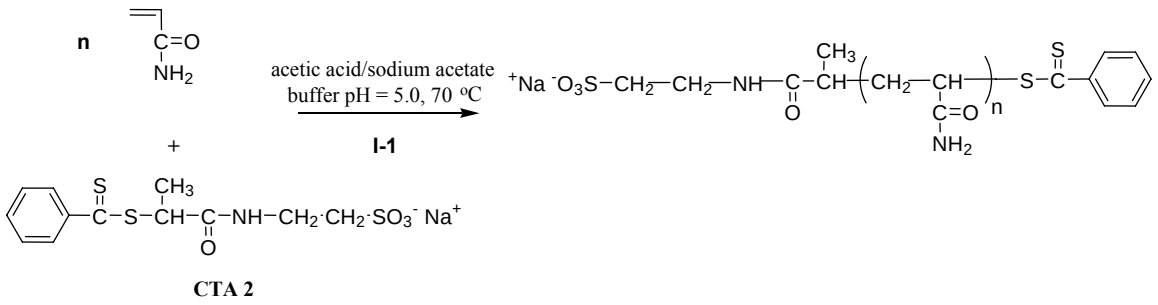

CTA 2

Scheme 2. Reaction scheme for the successful RAFT polymerization of acrylamide to produce macroCTA's of narrow molecular weight distribution with functional chain ends. The CTA **CTA-2** was used for its solubility in the acidic conditions necessary for control of the polymerization.

In order to further demonstrate the "livingness" of acrylamide (**M1**) polymerization under these conditions, a polyacrylamide macro-chain transfer agent (macroCTA) was prepared (M_n = 2.03 x 10^4, PDI = 1.03), isolated by dialysis, and lyopholized to yield an orange powder. A polymerization solution was then prepared as before utilizing this macroCTA as the chain transfer agent. Chain extension occurred with near-quantitative blocking efficiency, and indicated that nearly all of the polyacrylamide macroCTA chain ends remained active.

MacroCTAs prepared under these conditions, or those similar to the ones reported here should allow synthesis of block copolymers and other complex polymer architectures containing polyacrylamide subunits. Interestingly, the experimental molecular weights for these polymers, as determined by on-line MALLS, proved to be substantially higher than those predicted theoretically (see Table 4). Further, the very slow rate of polymerization combined with dithioester hydrolysis limited the conversion under these conditions to 28 %. Both the molecular weight deviation and the polymerization rate have been studied further and addressed.

In summary, optimal conditions for the aqueous RAFT polymerization of acrylamide (**M1**) in water were determined. These conditions afforded excellent control of the RAFT polymerization of acrylamide directly in aqueous media and are summarized in Table 4. Near quantitative chain extension and low polydispersities confirmed retention of the dithioester end groups during polymerization. MacroCTA's prepared under these conditions, or those similar to the ones reported here should allow synthesis of block copolymers and other complex polymer architectures containing polyacrylamide subunits

Section II.

Stimuli responsive copolymers of sodium 2-acrylamido-2-methylpropanesulfonate (AMPS) (**M4**) and sodium 3-acrylamido-3methylbutanoate (AMBA) (**M5**) were synthesized using reversible addition fragmentation chain transfer (RAFT) polymerization and their self assembly behavior was investigated utilizing ^{1}H NMR spectroscopy, dynamic light scattering, and fluorescence spectroscopy. More specifically,

the effects of block length and solution pH on the aggregation sizes of these reversible micelle-forming polymer surfactants were examined. The "A" block (corona of the micelle) was comprised of AMPS (**M4**) and the pH responsive "B" block (core of the micelle) that is tunable hydrophilic/hydrophobic was comprised of AMBA (**M5**). AMPS was used as a macroCTA for subsequent RAFT copolymerizations with AMBA. The length of the AMBA block was systematically varied in order to study the effects of copolymer composition on the self-assembly of the resulting copolymers in aqueous solutions as a function of pH (Scheme 3). Table 5 summarizes the results obtained from the analysis of the block and statistical copolymers by ASEC and ^{1}H NMR spectroscopy.

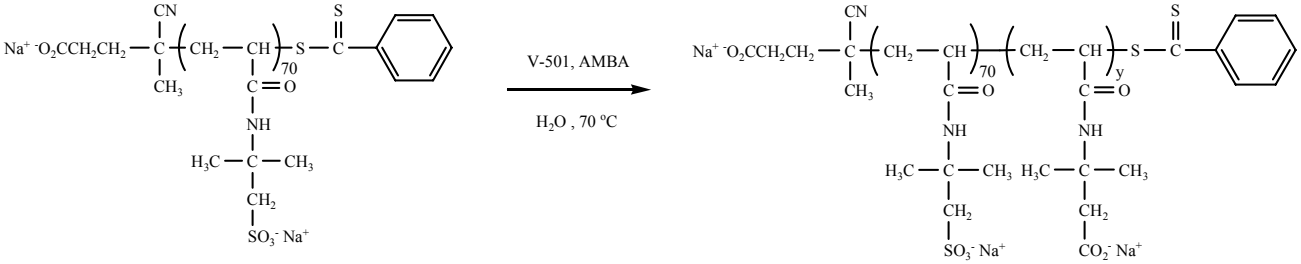

Scheme 3. Synthetic outline for the preparation of block copolymers of AMPS and AMBA via aqueous RAFT polymerization.

Table 5. Data for the RAFT Polymerization of AMBA Employing a PAMPS MacroCTA in Water (pH 8) at 70 °C with a [MacroCTA]/[Initiator] Ratio of 5/1 (Mole Basis); [**I-2**] = 2.84 mM, Time = 6 h.

	conv (%)[a]	M_n (theory)[b] (g/mol)	M_n (expt)[c] (g/mol)	M_w/M_n[c]	DP_{AMPS}	DP_{AMBA}	comp ASEC[c] (AMPS/AMBA)	comp NMR[e] AMPS/AMBA
P(AMPS$_{70}$-*b*-AMBA$_{62}$)	87	28 300	29 000	1.15	70[c]	62[c]	53/47	50/50
P(AMPS$_{70}$-*b*-AMBA$_{40}$)	85	24 200	24 500	1.10	70[c]	40[c]	64/36	64/36
P(AMPS$_{70}$-*b*-AMBA$_{25}$)	84	21 300	21 300	1.15	70[c]	25[c]	75/25	77/23
P(AMPS$_{70}$-*b*-AMBA$_{16}$)	94	19 600	19 700	1.21	70[c]	16[c]	82/19	82/19
P(AMPS$_{106}$-*stat*-AMBA$_{40}$)	84	28 700	32 000	1.15	106[d]	40[d]	-	73/27
P(AMPS$_{35}$-*stat*-AMBA$_{112}$)	89	27 100	29 800	1.14	35[d]	112[d]	-	24/76
P(AMPS$_{79}$-*stat*-AMBA$_{89}$)	87	29 400	35 300	1.13	79[d]	89[d]	-	47/53

[a] Determined from the residual monomer concentration obtained from the RI detector during ASEC.
[b] Determined using M_n(theory) = [M] x [MW_{mon}] x conversion / [CTA] + $MW_{MacroCTA}$.
[c] Determined by ASEC. [d] Determined by using the M_n determined from ASEC and the copolymer composition determined by ^{1}H NMR spectroscopy.
[e] Determined using ^{1}H NMR spectroscopy.

DLS was employed to characterize solutions of the copolymers in water at pH 9.0 and 1.0 (Table 6). The intensity-average hydrodynamic diameter (D_h) values obtained at high pH were in the region expected for molecularly dissolved polymers. A marked increase in D_h at pH 1.0 was observed for the block copolymer which indicated micelle formation. Importantly, aggregation was reversible as evidenced by alternation between unimers and micelles of specific sizes being observed during pH hysteresis experiments. The results from DLS, coupled with those obtained by ^{1}H NMR spectroscopy for the block copolymer solutions, were consistent with the reversible formation of uniform micelle-like structures with AMPS (**M4**) coronas and dehydrated AMBA cores (**M5**). The average aggregate diameters increased with increasing length of the AMBA (**M5**) block. This would be expected since it has been previously reported that the hydrophobic block controls the association behavior of amphipathic block copolymers in aqueous solutions.[15] Additionally, because of the polyelectrolyte nature of the AMPS-AMBA copolymers, the aggregation behavior was expected to be dependent on the ionic strength of the surrounding medium.

Table 6. Hydrodynamic Diameters (D_h) and Size Distribution Polydispersities (**ρ**) as Determined by DLS of Block and Statistical Copolymers of AMPS and AMBA as a Function of Solution pH.

sample	D_h (nm)		ρ
	pH 9.0	pH 1.0	pH 1.0
PAMPS$_{70}$	5	4	0.07
P(AMPS$_{70}$-*b*-AMBA$_{62}$)	6	25	0.11
P(AMPS$_{70}$-*b*-AMBA$_{40}$)	5	24	0.14
P(AMPS$_{70}$-*b*-AMBA$_{25}$)	6	21	0.11
P(AMPS$_{70}$-*b*-AMBA$_{16}$)	6	18	0.12
P(AMPS$_{106}$-*stat*-AMBA$_{40}$)	11	7	0.10
P(AMPS$_{35}$-*stat*-AMBA$_{112}$)	11	9	0.08
P(AMPS$_{79}$-*stat*-AMBA$_{89}$)	13	9	0.06

Statistical copolymers exhibited a slight decrease in D_h as the solution pH is lowered. Several explanations can be offered for this behavior. Because a majority of the AMBA (**M5)** units were ionized at pH 9.0, the statistical copolymers existed as polyelectrolytes. As the pH was lowered, AMBA (**M5)** units were protonated, leading to a lower effective charge density and reduced electrostatic repulsion. This would result in the copolymer collapsing to yield a smaller D_h. The decrease in D_h might also be attributed to intramolecular aggregation of the hydrophobic AMBA units at pH 1.0. Finally, because of the higher ionic strength of the solution at pH 1.0 as compared to pH 9.0, the polyelectrolyte effect should have caused a smaller D_h for the copolymers at the former pH.

In summary, a PAMPS macroCTA was employed in the synthesis of a series of well-defined AB diblock copolymers of AMPS and AMBA. Statistical copolymers of these two monomers were also prepared via aqueous RAFT. Excellent control of the molecular weight and molecular weight distributions was attained. Aqueous solution studies of a series of block and statistical copolymers employing ^{1}H NMR spectroscopy, DLS, and fluorescence spectroscopy indicated that these AB diblock copolymers can undergo self-assembly in solution below pH 5.5 to form reversible, pH-induced polymeric micelles with dehydrated AMBA cores capable of solubilizing low-molecular-weight organic molecules.

Section III.

N,*N*-dimethylvinylbenzylammonium chloride (DMVBAC, **M9**) and DMA (**M2**) were employed as macroCTAs for subsequent chain extension in order to prepare stimuli responsive block copolymers (Scheme 4).

It is well-known that when synthesizing AB diblock copolymers, especially for blocks comprised of monomers from two different families, that the order of polymerization can be extremely important. It was determined that chain extending a PDMA MacroCTA with DMVBAC (**P2-P4** in Table 7) led to the formation of well-defined block copolymers. High blocking efficiencies were observed with the resulting AB diblock copolymers having unimodal and narrow molecular weight distributions.

Table 7. Results from the Aqueous RAFT Block Copolymerizations of DMA and DMVBA.

	Conv[a] (%)	M_n **Theory**[b] (g/mol)	M_n ***ASEC***[c] (g/mol)	***PDI*** ***ASEC***[c]	M_n **NMR/ MALLS**[d] (g/mol)	**DP DMA**	**DP DMVBA**	**Composition (DMA/DMVBA)**[e]
PDMVBA MacroCTA	60	5 900	6 700	1.12	-	-	34[c]	-
P(DMVBA$_{34}$*-b-*DMA$_{46}$)	74	9 500	11 300	1.12	-	46[c]	34[c]	-
PDMA MacroCTA (P1)	24	4 800	4 900	1.17	6 600	67[d]	-	100 / 0
P(DMA$_{67}$*-b-*DMVBA$_{34}$)	61	10 800	12 100	1.20	13 270	67[d]	34[d]	67 / 33
P(DMA$_{67}$-*b*-DMVBA$_{50}$)	51	14 000	14 300	1.17	16 370	67[d]	50[d]	58 / 42
P(DMA$_{67}$-*b*-DMVBA$_{74}$)	70	18 100	14 900	1.17	21 150	67[d]	74[d]	48 / 52

[a] Determined from the residual monomer concentration obtained from the RI detector during ASEC.

[b] Determined using M_n(theory) = [Monomer] x [MW_{mon}] x conversion / [CTA] + $MW_{macroCTA}$.

[c] Determined by ASEC with three columns calibrated with poly(2-vinylpyridine) (P2VP) standards. Mobile phase: 1 wt% acetic acid/0.1 M Na_2SO_4, flow rate = 0.3 mL/min. Detectors included a UV-Vis and RI detector.

[d] Calculated by combining (1) the copolymer composition determined by ^{1}H NMR spectroscopy conducted in D_2O/DCl and (2) the molecular weight of the PDMA macroCTA determined by MALLS.

[e] Determined by ^{1}H NMR spectroscopy conducted in D_2O/DCl.

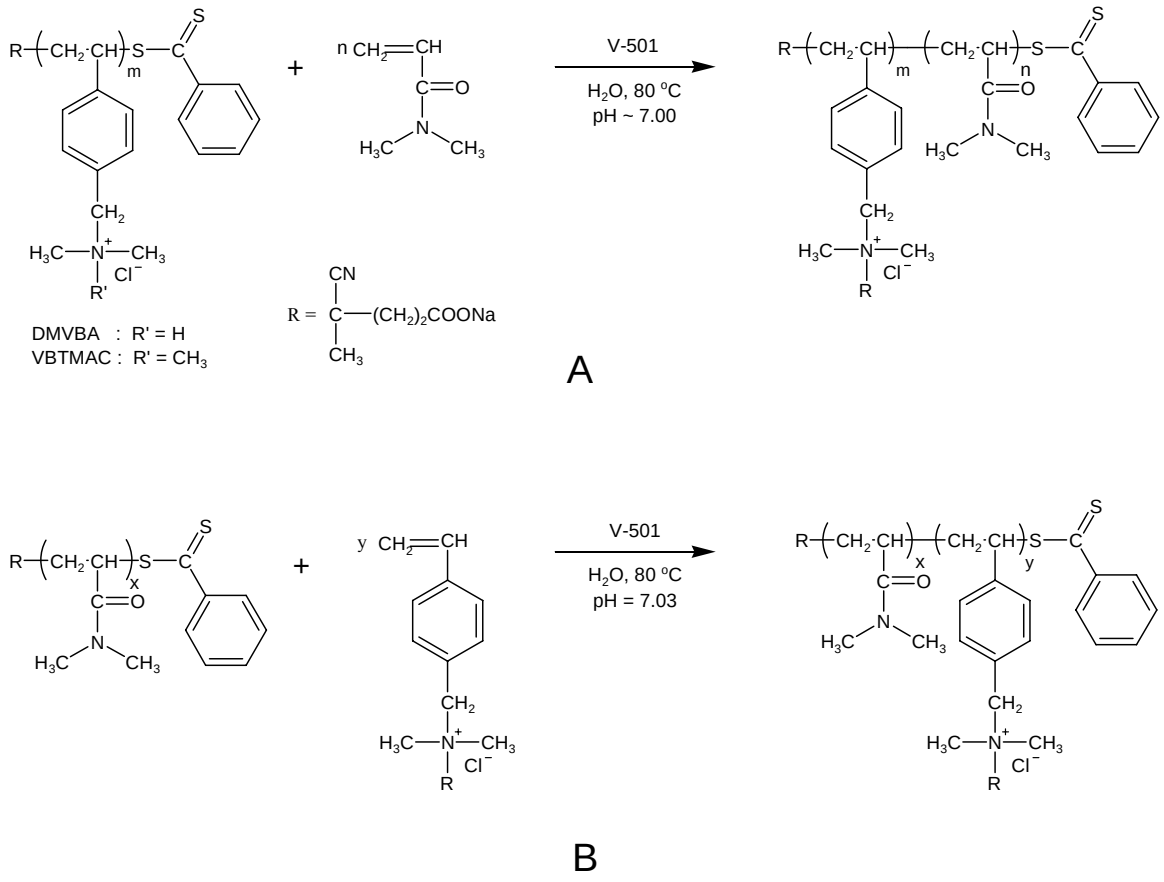

Scheme 4. Synthesis of a diblock copolymer of DMA and DMVBAC or VBTAC employing (**A**) a DMVBAC or VBTAC macroCTA and (**B**) a PDMA macroCTA.

The aqueous self-assembly behavior of the pH-responsive block copolymers, **P2-4** were investigated. PDMVBA possess a pK_a ~ 8.0 and is therefore hydrophobic under highly basic conditions. The block copolymers were first molecularly dissolved and the pH was adjusted to 1.0 ± 0.3. Under these conditions the block copolymers existed as single, isolated, molecularly dissolved chains, or "unimers". When the pH was raised above the critical value (pH ≈ pK_a), the DMVBA (**M6**) blocks became hydrophobic, and the block copolymers self-assembled forming micelle-like structures. DLS was utilized to characterize the copolymer solutions in water at pH 1 and 10 (Table 8). The intensity-average hydrodynamic diameters (D_h) obtained at low pH were in the range expected for molecularly dissolved polymers with the molecular weights considered, i.e 5-6 nm. A marked increase in D_h at pH 10 was observed for the block copolymer systems (D_h = 22-69 nm). The micelle diameters increased with increasing length of the DMVBA block. This would be expected since the hydrophobic block controls the association behavior of amphipathic block copolymers in aqueous solutions.

Table 8. Hydrodynamic Diameter (D_h) and Polydispersity Determined by DLS at pH 1.0 and 10.0 for the PDMA MacroCTA and Block Copolymers with DMVBA.

	D_h (nm)		
	pH 1.0	**pH 10.0**	ρ
PDMA MacroCTA	3	4	0.06
P2	5	22	0.16
P3	6	50	0.11
P4	6	69	0.14
P3X	101	59	0.18

In addition to providing pH-responsive behavior, the tertiary amine groups of the DMVBA (**M6**) block can also be utilized to selectively crosslink the core of the polymeric micelles. As a representative example, **P3** micelles were crosslinked by the addition of α,α'-dibromo-*p*-xylene. Due to its inherent hydrophobicity, the crosslinking agent would be expected to partition into the micelle cores, thus facilitating the potential for intermolecular linkage between the tertiary amine groups of adjacent chains. Due to intermolecular covalent bonding between core chains, crosslinked micelles are not capable of dissociating to their respective unimeric states.

The synthesis and solution characterization of a novel series of AB diblock copolymers with neutral, water-soluble acrylamido-based A blocks (DMA) (**M2**) and pH-responsive styrenic B blocks (DMVBA) (**M6**) have been accomplished. In order to yield well-defined block copolymers of DMA and DMVBA with minimal homopolymer impurity, it was necessary to polymerize DMA first and use this as a macroCTA for the block copolymerization of DMVBA. Due to the stimuli-responsive nature of the DMVBA block, reversible aggregation of these block copolymers was demonstrated. Additionally, core-crosslinked micelles were also obtained by the addition of a difunctional crosslinking agent to a micellar solution of the block copolymer. The cross-linked micelles remain as intermolecular aggregates at low pH.

Section IV.

Building on earlier results, the aim of this work was to impart better control for the RAFT polymerization of DMA (**M2**). To accomplish this, two novel CTAs (**CTA-6**, **CTA-7**) were synthesized to be possess an R leaving group structurally and electronically similar to that of DMA. Experiments were conducted to determine the efficiency of **CTA 3** and **CTA-7** in mediating the molecular weight and controlling the polydispersity of DMA (**M2**). The M_{nSEC} values as determined by SEC using a MALLS detector were considered absolute. These results, along with the polydispersity indices (PDIs), are summarized in Table 9. For both polymerizations, the experimentally observed molecular weights were consistently higher than those predicted by theory; however, better agreement was observed with the monofunctional **CTA-6**.

Table 9. Experimental Data from the RAFT Polymerization of DMA with **CTA-6** (Target MW = 23K) and **CTA-7** (Target MW = 46K) in d_6-Benzene (60 ^oC) [DMA] = 1.95 M, [CTA] = 8.52×10^{-3} M (1) and 4.27×10^{-3} M (2), [**I-3**] = 8.48×10^{-4} M.

CTA	[CTA]/[I]	*Time* (min)	% Conv [a]	MW_{Th} [b]	$M_{n\ SEC}$ [c]	M_w/M_n [c]
6	10	540	30	6,900	8,800	1.16
6	10	720	38	8,800	9,900	1.11
6	10	1,080	52	11,900	13,000	1.07
6	10	1,380	57	13,000	15,900	1.09
7	5	1,080	17	7,900	13,100	1.14
7	5	1,560	36	16,500	20,300	1.17
7	5	1,920	46	21,200	28,400	1.17

[a] As determined by ^1H NMR spectroscopy in d_6-benzene. [b] SEC in DMF at room temperature, flow rate of 0.5 mL/min, with x2 PL Mixed D columns, PL UV1200, Optilab RI, and DAWN EOS detectors. [C] These values represent those determined for the unimodal or multimodal distributions where applicable.

After establishing the polymerization kinetics and molecular weight dependence using **CTA-6** and **CTA-7**, a series of PDMA homopolymers of varying molecular weights and functionality were synthesized as macroCTAs for tailoring specific hydrophilic di- and triblock copolymer architectures. The macroCTAs **PDMA1**, **PDMA2**, and **PDMA3** were synthesized in benzene. Using **CTA-6**, monofunctional PDMA homopolymers were synthesized (**PDMA1** and **PDMA2**) and using **CTA-7** a difunctional PDMA homopolymer was synthesized (**PDMA3**). The molecular weights and PDI values

obtained by SEC-MALLS in aqueous media are listed in Table 10. In addition to the PDMA macroCTAs, a polysulfobetaine macroCTA (**PSB**) was synthesized directly in aqueous salt solution. The molecular weight and polydispersity values for **PSB** are also listed in Table 10.

Table 10. Conversion, Molar Mass, and Polydispersity Data for the PDMA (**PDMA1-PDMA3**) and PMAEDAPS (**PSB**) MacroCTAs.

Polymer	**CTA**	**[CTA]/[I]**	**Time (min)**	**Conv [a] (%)**	**MW_{Th}**	**M_{nSEC} [b]**	**M_w/M_n**
PDMA1	6	5	1,030	39	10,140	10,700	1.04
PDMA2	8	5	700	51	23,300	32,000	1.07
PDMA3	7	5	1,600	51	23,370	26,000	1.14
PSB	1	5	480	65	29,300	39,150	1.25

[a] As determined by gravimetric analysis. [b] ASEC in 0.5 M NaBr/Acetonitrile (80/20:v/v) at room temperature, flow rate of 0.5 mL/min, with x1 Viscotek G4000 column, PL UV1200, Optilab RI, and DAWN EOS detectors.

Depicted in Scheme 5 are the strategies employed for the synthesis of the desired di- and triblock polymer architectures. The DMA/MAEDAPS diblock copolymers **B1** and **B2** were synthesized using the mono- and difunctional macroCTAs **PDMA1** and **PDMA2** (Scheme 5a). To obtain the MAEDAPS-DMA-MAEDAPS triblock copolymer, the difunctional macroCTA **PDMA3** was employed in a similar fashion, as shown in Scheme 5b. In addition, a fourth block copolymer was synthesized in a reverse procedure in which **PSB** was used for the polymerization of DMA (Scheme 5c). The block copolymers are summarized in Table 11.

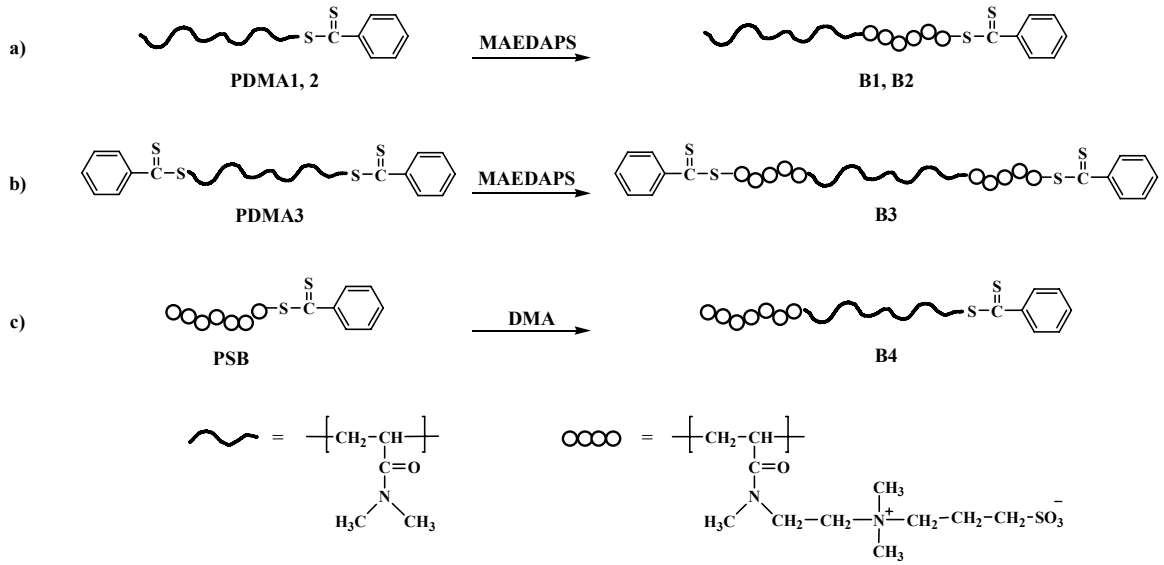

Scheme 5. Synthesis of P(DMA-*b*-MAEDAPS) (**B1-B2**) (a) P(MAEDAPS-*b*-DMA-*b*-MAEDAPS) (**B3**) (b), and P(MAEDAPS-*b*-DMA) (**B4**) (c).

Table 11. Conversion, Molar Mass, Polydispersity, and Composition Data for the DMA-MAEDAPS and MAEDAPS-DMA Block Copolymers.

Copolymer	Macro-CTA	Comonomer	Conv [a] (%)	MW_{Th}	M_{nSEC} [b]	M_w/M_n	Mol % DMA (SEC) (calc)	Mol % DMA (NMR) [c]
B1	PDMA1	MAEDAPS	98	33,000	69,800	1.34	34	65
B2	PDMA2	MAEDAPS	98	54,100	63,600	1.40	74	77
B3	PDMA3	MAEDAPS	99	70,200	72,400	1.81	61	58
B4	PSB	DMA	67	65,800	70,800	1.41	69	65

[a] As determined by monitoring the loss of monomer area in the ASEC chromatograms [b] ASEC in 0.5 M NaBr/Acetonitrile (80/20:v/v) at room temperature, flow rate of 0.5 mL/min, with x1 Viscotek G4000 column, PL UV1200, Optilab RI, and DAWN EOS detectors. [c] As determined by degated ^{13}C NMR spectroscopy.

Dynamic light scattering (DLS) measurements were conducted to determine the hydrodynamic diameter of polymers/aggregates in salt and pure water. These experiments were performed in either 0.5 M NaCl or DI water at 25 ^{o}C at a polymer concentration of 1 g/dL. Shown in Table 12 are the polydispersities (ρ) and the sizes of the unimers and aggregates determined by CONTIN for block copolymers **B1-B3.** The unimer sizes for all three block copolymers in salt water were of the same order (14-17 nm) with polydispersities less than 0.17. The similarity of the observed hydrodynamic diameters of the unimers should have been expected since all three copolymers exhibit similar retention volumes in the ASEC chromatograms. It was noted that the diameters obtained by CONTIN analysis in NaCl were determined assuming a spherical geometry; however, poor solvation of the MAEDAPS block may have led to more complex

geometries including coil/blobs, loops, or dumbbells depending on the copolymer topology.

In DI water, both diblock copolymers **B1** and **B2** underwent self-assembly, which resulted in aggregates with apparent hydrodynamic diameters of 71 nm, and 63 nm, respectively. The smallest aggregates were observed for **B2.** This might be expected since larger coronal chains and smaller associative blocks typically promote smaller aggregation numbers due to entropic penalties arising from chain crowding/stretching of both corona and core blocks. The slightly larger sizes observed for **B1**, which contained shorter coronal chains and longer core chains, may reflect higher aggregation numbers due to less steric crowding of the coronal chains and greater core interactions. Since **B1** more closely resembled 'crew-cut' systems, spherical morphology cannot be implied. A proposed model for micelle formation of **B1** and **B2** is depicted in Scheme 3A.

For the triblock copolymer **B3**, the narrow/unimodal size distribution indicated the formation of flower-like micelles, suggesting closed associations (depicted in Scheme 3B). This system exhibited the largest aggregates with an average hydrodynamic diameter of 93 nm. These results were interesting since back-folding of the coronal chains can promote smaller micelle sizes. When comparing **B2** and **B3**, the higher overall MADAEPS content of **B3** may have promoted larger cores, leading to larger aggregate sizes. Further studies regarding aggregation behavior of these systems as influenced by polymer concentration, relative block length sizes, and topology are ongoing in our laboratory.

Table 12. DLS Data for the DMA-MAEDAPS diblock (**B1** and **B2**) and the MAEDAPS-DMA-MAEDAPS triblock (**B3**) copolymers in 0.5 M NaCl and in DI H_2O.

Copolymer	***Repeat Units***	**d_h (nm)[a]**	**ρ[b]**	**d_h (nm)[a]**	**ρ[b]**
	MAEDAPS:DMA:MAEDAPS	**NaCl**		**H_2O**	
B1	210 : 110 : -	14	0.09	71	0.06
B2	110 : 320 : -	15	0.16	63	0.11
B3	80 : 260 : 80	17	0.15	93	0.07

[a] Intensity average hydrodynamic diameters [b] **ρ** = polydispersity index = μ_2/Γ^2

In this work we have demonstrated the efficiency of a novel bi-functional, amide-based CTA, **CTA-7**, for the RAFT polymerization of DMA in benzene. This new CTA was evaluated in comparative studies with the monofunctional **CTA-6**. Although **CTA-7** resulted in slightly higher polydispersities, the molecular weight control was comparable to that of **CTA-6**. Also, a long induction period was associated with **CTA-7**. Optimized reaction conditions were then utilized to tailor mono and difunctional DMA macroCTAs, which were subsequently used for the RAFT block copolymerization of a sulfobetaine monomer, MAEDAPS, in aqueous media. In addition, a sulfobetaine macroCTA was

synthesized and used for the aqueous RAFT polymerization of DMA. Preliminary studies regarding the self-assembly of the AB and BAB hydrophilic block copolymers in aqueous media were also conducted. Our results indicated the formation of well-defined aggregates including 'star-like' or 'flower-like' micelles with varying sizes dependent on block copolymer topology. This work represented the first example of the synthesis and solution characterization of sulfobetaine containing triblock copolymers.

Section V.

N-Isopropyl acrylamide (NIPAM, **M3)** is an important temperature-responsive monomer and was therefore chosen for incorporation into temperature-responsive copolymers under a range conditions. Initial studies demonstrated the polymerization of this monomer under organic conditions, while later experiments demonstrated the polymerization of this monomer under aqueous conditions. The results for the homopolymerization of NIPAM (**M3**), under those conditions outlined in Scheme 6, are summarized in Table 13. From Table 13 it can be concluded that the polymerization conditions provided good control for NIPAM (**M3**) homopolymerizations.

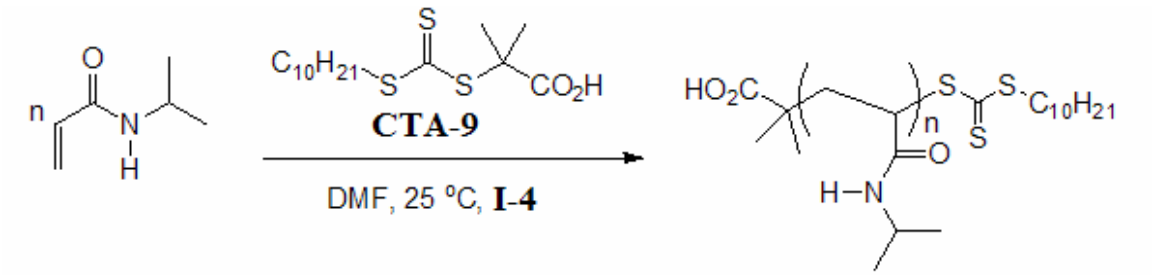

Scheme 6. Synthetic pathway for the room temperature RAFT polymerization of N-isopropylacrylamide in DMF.

Table 13. Conversion, molar mass, and polydispersity data for NIPAM homopolymerizations in DMF.

Sample[a]	time (h)	Conversion (%)[b]	$[CTA]_o/[I]_o$	M_n (theory)	M_n (expt)[c]	PDI
NIPAM1	6	39	20	20 400	24 000	1.04
NIPAM2	12	58	20	30 600	33 000	1.05
NIPAM3	24	74	20	38 600	40 000	1.05
NIPAM4	6	52	10	27 500	31 000	1.03
NIPAM5	12	70	10	37 000	37 000	1.06
NIPAM6	24	86	10	45 000	43 000	1.03
NIPAM7	6	62	5	32 600	29 200	1.07
NIPAM8	12	77	5	40 700	40 000	1.06
NIPAM9	24	90	5	47 000	44 500	1.06

[a] Polymers synthesized at 25 °C at 33 wt % monomer in DMF ($[CTA]_o/[M]_o$: 1/465) under a nitrogen atmosphere with **I-4** as the initiator and **CTA-9**. [b] Conversions were determined by comparing the area of the RI signal of the monomer at t_o to that at t_x. [c] As determined by SEC (0.5 mL/min, 60 °C, Polymer Labs PL gel 5 μm mixed C column, DMF eluent).

After establishing favorable conditions for the RAFT mediated homopolymerization of NIPAM (**M3**), blocking studies were conducted. PNIPAM macroCTA was synthesized and subsequently chain extended with additional NIPAM (**M3**) monomer under experimental conditions identical to those reported above for the homopolymerizations in DMF. Near-quantitative blocking efficiency (percent macroCTA converted to 'diblock' copolymer) was confirmed. Additionally, a lack of significant homopolymer impurity, as evidenced by the absence of a detectable low molecular weight polymer, suggested that most of the PNIPAM macroCTA retained the trithiocarbonate functionality at the chain terminus.

NIPAM was polymerized in D_2O over selected time intervals using **I-5** as the free radical initiator and **CTA-5** or **CTA-10** as the RAFT CTA (Scheme 2). Experimental data for the homopolymerizations of NIPAM (**M3**) are summarized in Table 14. The results presented in Table 14 indicate that the polymerization conditions afforded the controlled homopolymerization of NIPAM (**M3**).

Table 14. Conversion, molar mass, and polydispersity data for the aqueous RAFT polymerization of N-isopropylacrylamide (NIPAM) at 25 °C mediated by **CTA-5** and **CTA-10** with initial CTA:initiator and monomer:CTA ratios of 3:1 and 600:1, respectively.

Sample No.	CTA[a]	Time (min.)	% Conv.[b]	M_n[b] $\left(\frac{g}{mol}\right)$	M_n Theory $\left(\frac{g}{mol}\right)$	M_w/M_n[b]
1	**5**	90	22	22 600	15 200	1.32
2	**5**	180	55	45 800	37 600	1.09
3	**5**	300	75	61 600	51 200	1.07
4	**5**	525	89	73 000	60 700	1.06
5	**10**	90	25	21 200	17 300	1.15
6	**10**	210	54	44 500	37 000	1.05
7	**10**	360	72	59 400	49 200	1.05
8	**10**	720	88	76 200	60 000	1.03

[a] Polymers synthesized at 25 °C at 0.5 M monomer in D_2O($[CTA]_o/[M]_o$:1/600) under a nitrogen atmosphere with **I-5** as the initiator. [b] Conversions were determined using ^1H NMR spectroscopy by comparing the area of the vinyl proton resonances to the total methyne signal. [c] As determined by ASEC[0.5 $mL \cdot min^{-1}$, 25 °C, Viscotek TSK Viscogel columns G3000 PWXL (,50 000 $g \cdot mol^{-1}$, 200 Å) and G4000 PWXL (2000-300 000 $g \cdot mol^{-1}$, 500 Å), 0.1 M $NaNO_3$ (aqueous) eluent].

After having established conditions for the room temperature polymerization of NIPAM in water, homopolymers of DMA (**M2**) were synthesized using **CTA-5** and **CTA-10** as the RAFT agents to yield the corresponding mono- and difunctional macroCTAs (Scheme 6). The resulting monofunctional and difunctional polyDMA macroCTAs were then used for the subsequent RAFT block copolymerization of NIPAM (Scheme 6) to yield a range of di and tri block copolymers. The molecular weight and polydispersity values are listed in Table 15.

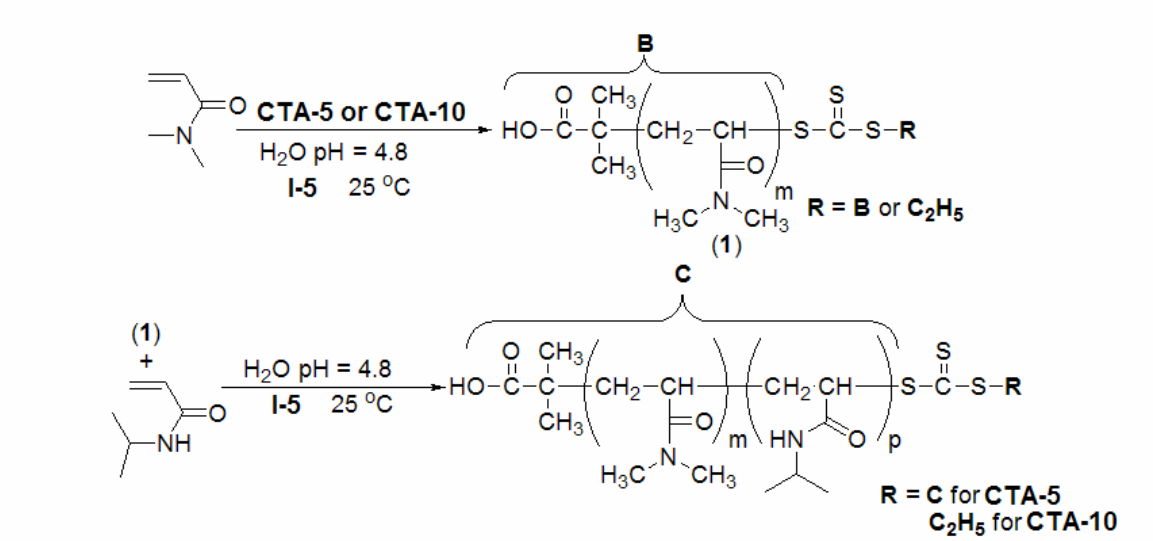

Scheme 7. Synthetic route for preparation of di- and triblock copolymers of DMA and NIPAM *via* aqueous room temperature RAFT.

Table 15. Molecular weight, composition, and polydispersity data for di- and triblock copolymers DMA (A block) and NIPAM (B block) synthesized in the presence of **CTA-5** and **CTA-10**.

Sample Number	Polymer Type	Polym. Time (min.)	DP DMA[a]	DP NIPAM[b]	Molar % NIPAM	MW[b] $\left(\frac{g}{mol}\right)$	M_w/M_n[a]
1	ABA	45	106	77	42	19200	1.13
2	ABA	120	106	197	65	32800	1.04
3	ABA	180	106	273	72	41300	1.03
4	ABA	300	106	376	78	53000	1.14
5	AB	45	100	71	42	17900	1.11
6	AB	120	100	174	64	29600	1.15
7	AB	240	100	254	71	38600	1.12
8	AB	360	100	460	82	61900	1.21

[a] As determined by ASEC[0.5 mL·min^{-1}, 25 °C, Viscotek TSK Viscogel columns G3000 PWXL (,50 000 g·mol^{-1} , 200 Å) and G4000 PWXL (2000-300 000 g·mol^{-1}, 500 Å), 0.1 M $NaNO_3$ (aqueous) eluent]. [b]Determined by ^{1}H NMR spectroscopy in D_2O

The next objective of this study was to systematically vary the length of the NIPAM blocks in order to study the effect of copolymer composition on the temperature-induced micellization for AB and ABA DMA/NIPAM block copolymers. Temperature-induced micellization could be followed by monitoring changes in polymer hydrodynamic volume using dynamic light scattering. Diblock copolymer solutions showed the expected

transition from molecularly dissolved unimers at low temperatures to aggregated micelles above a critical micelle temperature (CMT). As the solution temperature was raised above the CMT, micelle hydrodynamic diameters begin to decrease. The triblock polymer solutions, in contrast, exhibited temperature induced association to form micelles only at longer NIPAM block lengths; the smaller triblock polymers remained molecularly dissolved as unimers. Both the di- and triblock copolymer micelles have, however, showed increasing sizes along with decreasing CMTs as the NIPAM block length increases. The observed block length dependent CMTs were also in agreement with results from the T_2 experiments.

Results from static light scattering experiments along with unimer and micelle sizes are summarized in Table 16. For both the di- and triblock copolymers, there was a clear increase in both micelle size and molecular weight as the NIPAM block length was increased. While both di- and triblock copolymers systems showed a general increase in the aggregation number with increasing NIPAM block length, aggregation numbers and sizes for the diblocks were considerably larger than those of triblocks with similar compositions. Clearly, block structure has a large influence on the micelle sizes and molecular weights as well as the CMTs.

Table 16. Hydrodynamic Diameter (D_h), Critical Micelle Temperatures (CMT), Micelle Molecular weights (M_w), aggregation numbers (N_{agg}), and second virial coefficient (A_2) determined by Static and dynamic light scattering as a function of temperature.

Sample	D_h 25°C[a] (nm)	D_h 45°C[a] (nm)	CMT[a] $(^\circ C)$	M_w *10^{-6}[b] $\left(\frac{g}{mol}\right)$	$A_2\times10^4$ $\left[\frac{mL\bullet mol}{g^2}\right]$	N_{agg}[c]
$DMA_{53}NIPAM_{77}DMA_{53}$	5.0	4.2	-	-	-	-
$DMA_{53}NIPAM_{197}$ DMA_{53}	7.3	4.8	-	-	-	-
$DMA_{53}NIPAM_{273}$ DMA_{53}	7.5	14.5	41.5	0.59	3.78	14
$DMA_{53}NIPAM_{376}$ DMA_{53}	9.8	28.0	37.5	3.20	2.58	25
$DMA_{100}NIPAM_{71}$	6.3	22.0	44.0	1.36	3.03	68
$DMA_{100}NIPAM_{174}$	7.2	31.0	37.3	3.52	1.11	103
$DMA_{100}NIPAM_{254}$	9.7	31.0	36.4	6.63	1.14	152
$DMA_{100}NIPAM_{460}$	10.5	76.0	34.6	15.94	1.10	213

[a]Dynamic light scattering studies of the block copolymer micelles in aqueous solution were conducted using an Malvern Instruments Zetasizer Nano series instrument equipped with a 22 mW He-Ne laser operating at $\lambda = 632.8$ nm, an avalanche photodiode detector with high quantum efficiency, and an ALV/LSE-5003 multiple tau digital correlator electronics system at a polymer concentration of 1.00 g / L. [b]Static light scattering measurements were performed at 50 °C on a Malvern Instruments Zetasizer at a constant scattering angle of 137 degrees. [c]Determined from the relations $N_{agg} = MW_{micelle} / MW_{unimer}$

In this work we have demonstrated the ability to conduct the RAFT polymerization of NIPAM (**M3**) at room temperature, in DMF. We have also shown that PNIPAM may be synthesized in water at room temperature using the RAFT process. A series of di- and triblock copolymers with constant hydrophilic block lengths and variable NIPAM block lengths was then synthesized in order to systematically study the temperature-dependent micellization. Micelle sizes and molecular weights determined by a combination of dynamic and static light scattering experiments showed a general increase with increasing NIPAM block length. This trend was observed for both di- and triblock copolymers, however micellization in the latter was only observed at longer NIPAM block lengths. We believe that this represents a significant advance in terms of both the facile synthesis and characterization of NIPAM-based materials and will no doubt lead to the preparation of more structurally complex copolymers in the near future.

CONCLUSIONS & POTENTIAL

In summary, through ongoing research focusing on both Type I and Type II SMFPs, we have demonstrated the synthesis and behavior of materials that can respond *in situ* to stimuli (ionic strength, pH, temperature, and shear stress). We believe that these SMFPs have significant potential in EOR processes. Type I SMFPs have been shown to reversibly form micelles in water and have the potential to be utilized in applications that serve to lower interfacial tension at the oil/water interface, resulting in emulsification of oil. Type 2 SMFPs, which are high molecular weight polymers, have been synthesized and have prospective applications related to the alteration of fluid viscosity, and thus mobility, during the recovery process. With these technologically “smart” polymers, it should be possible to produce more of the original oil in place and a larger portion of that by-passed or deemed “unrecoverable” by conventional chemical flooding.

LIST OF SCHEMES, FIGURES AND TABLES

REFERENCES

(1) Lowe, A. B.; McCormick, C. L. *Chem. Rev.* **2002**, *102*, 4177-4189.
(2) Kathmann, E. L.; McCormick, C. L. In *Polym. Mat. Encycl.*; Salamone, J. C., Ed.; CRC Press: Boca Raton, FL, 1996; Vol. 7, pp 5462-5476.
(3) Salamone, J. C.; Rice, W. C. In *Encycl. Polym. Sci. Eng.*, 1987; Vol. 11, pp 514-530.
(4) Candau, F.; Joanny, J. F. In *Polym. Mat. Encycl.*; Salamone, J. C., Ed.; CRC Press: Boca Raton, FL, 1996; Vol. 7, pp 5462-5476.
(5) Galin, J.-C. In *Polym. Mat. Encycl.*; Salamone, J. C., Ed.; CRC Press: Boca Raton, FL, 1996; Vol. 10, pp 7189-7201.
(6) Kudaibergenov, S. E. *Polyampholytes: Synthesis, Characterization, and Application*; Plenum Corporation: New York, 2002.
(7) Bekturov, E. A.; Kudaibergenov, S. E. *Makromol. Chem., Macromol. Symp.* **1989**, *26*, 281-295.
(8) Bekturov, E. A.; Kudaibergenov, S. E.; Rafikov, S. R. *J. Macromol. Sci., Rev. Macromol. Chem. Phys.* **1990**, *C30*, 233-303.
(9) Higgs, P. G.; Joanny, J. F. *J. Chem. Phys.* **1991**, *94*, 1543-1554.
(10) Kantor, Y.; Li, H.; Kardar, M. *Phys. Rev. Let.* **1992**, *69*, 61-64.
(11) Dobrynin, A. V.; Rubinstein, M. *J. Physique II* **1995**, *5*, 677-695.
(12) Kudaibergenov, S. E. *Adv. Polym. Sci.* **1999** *144*, 115-197.
(13) Dobrynin, A. V.; Colby, R. H.; Rubinstein, M. *Macromolecules* **1995**, *28*, 1859-1871.
(14) Peiffer, D. G.; Lundberg, R. D.; Kowalik, R. M.; Turner, S. R. *U.S. Patent 4,460,758*, 1984.
(15) Peiffer, D. G.; Lundberg, R. D.; Turner, S. R. *U.S. Patent 4,461,884*, 1984.
(16) Peiffer, D. G.; Lundberg, R. D. *Polymer* **1985**, *26*, 1058-1068.
(17) Peiffer, D. G.; Lundberg, R. D. *U.S. Patent 4,710,555*, 1987.
(18) Salamone, J. C.; Ahmed, I.; Rodriguez, E. L.; Quach, L.; Watterson, A. C. *J. Macromol. Sci., Chem.* **1988**, *25*, 811-837.
(19) Neyret, S.; Candau, F.; Selb, J. *Acta Polym.* **1996**, *47*, 323-332.
(20) McCormick, C. L.; Salazar, L. C. *Polymer* **1992**, *33*, 4384-4387.
(21) Ohlemacher, A.; Candau, F.; Munch, J. P.; Candau, S. J. *J. Polym. Sci., Pt. B.: Polym. Phys.* **1996**, *34*, 2747-2757.
(22) McCormick, C. L.; Johnson, C. B. *Macromolecules* **1988**, *21*, 694-699.
(23) McCormick, C. L.; Johnson, C. B. *Polymer* **1990**, *31*, 1100-1107.
(24) McCormick, C. L.; Salazar, L. C. *J. Appl. Polym. Sci.* **1993**, *48*, 1115-1120.
(25) Fevola, M.J.; Ezell, R.G.; Bridges, J.K.; McCormick, C.L. *Polym. Prepr*. **2003**, *44(1)*, 1150-1151.
(26) Fevola, M.J.; Kellum, M.G.; Hester R. D.; McCormick, C.L. *J. Polym. Sci., Part A: Polym. Chem*. **2004**, *42*, 3256-3270.
(27) Fevola, M.J.; Kellum, M.G.; Hester R. D.; McCormick, C.L. *J. Polym. Sci., Part A: Polym. Chem*. **2004**, *42*, 3236-3251.
(28) McCormick, C. L. and Blackmon, K. P. *J. Polym. Sci. Pt. A: Polym Chem*. **1986**, *24*, 2635.
(29) McCormick, C. L. and Blackmon, K. P. U.S. Patent 4,584,358, 1986.

(30) Ezell, R.G.; Gorman, I.; Lokitz, B.; Ayres, N.; McCormick, C.L. *J. Polym. Sci., Part A: Polym. Chem*. **2006**, *44*, 3125-3139.
(31) Ezell, R.G.; Gorman, I.; Lokitz, B.S.; Treat, N.; McConaughy, S.; McCormick, C.L. *J. Poly. Sci. Pt. A: Poly. Chem.* **2006**, *44*, 4479-4493.
(32) McCormick, C. L. and Blackmon, K. P. U.S. Patent 4,649,183, 1987.
(33) K.S. Sorbie, *Polymer Improved Oil Recovery*, ***1*** 1991.
(34) P.H Doe and R.B. Needham, *Polymer Flooding Review* **1987**, 1503.
(35) Yusa, S.; Shimada,Y.; Mitsukami, Y.; Yamamoto, T.; Morishima, Y. Macromolecules 2004, 37, 7507.
(36) Virtanen, J.; Holappa, S.; Lemmetyinen, H.; Tenhu, H. Macromolecules 2002 35, 4763.
(37) Zhang, W.; Shi, L.; Wu, K.; An Y.; Macromolecules 2005 ASAP
(38) Liu, B.; Perrier, S. Journal of Polymer Science Part A, 2005, 43, 3643.
(39) Arotcarena, M.; Heise, B.; Ishaya, S.; Laschewsky, A.; Journal of the American Chemical Society 2002, 124, 3787.
(40) Virtanen, J.; Arotcarena, M.; Heise, B.; Ishaya, S.; Laschewsky, A.; Tenhu, H. Langmuir 2002, 18, 5360.
(41) Sumerlin, B. S.; Lowe, A. B.; Thomas, D. B.; McCormick, C. L Macromolecules 2003, 36, 5982.
(42) Sumerlin, B. S.; Lowe, A. B.; Thomas, D. B.; Convertine, A. J.; Donovan, M. S.; McCormick, C. L. J. Poly. Sci. Part A 2004, 42, 1724.
(43) Yu, K.; Bartels, C.; Eisenberg, A. Macromolecules 1998, 31, 9399.
(44) Zhang, L.; Eisenberg, A. Macromolecules 1999, 32, 2239.
(45) Hawker, C. J.; Bosman, A. W.; Harth, E. Chem. Rev. 2001, 101, 3661.
(46) Matyjaszewski, K.; Xia, J. Chem. Rev. 2001, 101, 2921.
(47) Moad, G.; Rizzardo, E.; Thang, S. H. Austr. J. Chem. 2005, 58, 379.
(48) Chiefari, J. ; Chong, Y. K.; Ercole, F.; Krstina, J.; Jeffery, J.; Le, T. P. T.; Mayadunne, R. T. A.; Meijs, G. F.; Moad, C. L.; Moad, G.; Rizzardo, E.; Thang, S. H. Macromolecules 1998, 31, 5559.
(49) Le, T. P.; Moad, G.; Rizzardo, E.; Thang, S. H. Int. Pat. 9801478 [Chem. Abstr. 1998, 128 115390f]
(50) Sumerlin, B. S.; Donovan, M. S.; Mitsukami, Y.; Lowe, A. B.; McCormick, C. L. Macromolecules 2001, 34, 6561.
(51) Vasilieva, Y. A.; Thomas, D. B.; Scales, C. W.; McCormick, C. L. Macromolecules 2004, 37, 2728.
(52) Donovan, M. S.; Lowe, A. B.; Sanford, T. A.; McCormick, C L. J. Polym. Sci., Part A: Polym. Chem. 2003, 41, 1262.
(53) Donovan, M. S.; Sumerlin, B. S.; Lowe, A. B.; McCormick, C. L. Macromolecules 2002, 35, 8663.
(54) Donovan, M. S.; Sanford, T. A.; Lowe, A. B.; Sumerlin, B. S.; Mitsukami, Y.; McCormick, C. L. Macromolecules 2002, 35, 4570.
(55) Donovan, M. S.; Lowe, A. B.; Sumerlin, B. S.; McCormick, C. L. Macromolecules 2002, 35, 4123.
(56) Thomas, D. B.; Sumerlin, B. S.; Lowe, A. B.; McCormick, C. L. Macromolecules 2003, 36, 1436.

ACRONYMS AND ABBREVIATIONS

A_2	second virial coefficient
AAL	N-acryloyl alanine
AAS	N-acryloyl aspartate
AIBN	2,2'-azobis(2-methylpropionitrile)
AM	acrylamide
AMBA	sodium 3-acrylamido-3-methylbutanoate
AMBATAC	poly(acrylamide-*co*-sodium 3-acrylamido-3-methylbutanoate-*co*-(3-acrylamidopropyl)trimethylammonium chloride)
AMDAP	poly(acrylamide-*co*-3-(3-acrylamidopropyldimethylammonio) propionate)
AMPS	sodium 2-acrylamido-2-methylpropanesulfonate
APTAC	(3-acrylamidopropyl)trimethyl ammonium chloride
ASEC	aqueous size exclusion chromatography
ATRP	atom transfer radical polymerization
AVA	N-acryloyl valine
CRP	controlled radical polymerization
CTA	chain transfer agent
D_h	hydrodynamic diameter
DI	deionized
DLS	dynamic light scattering
DMA	N,N-dimethyl acrylamide
DMF	N,N-dimethyl formamide
DMVBA	N,N-dimethylvinylbenzylamine

DMVBAC	N,N-dimethylvinylbenzylammonium chloride
DP	degree of polymerization
EOR	enhanced oil recovery
^{1}H NMR	proton nuclear magnetic resonance
k	rate constant
M	monomer
M_n	number average molecular weight
MAEDAPS	*3*-[2-(N-methylacrylamido)-ethyldimethylammonio] propane sulfonate
MALLS	multi-angle laser light scattering
MEHQ	hydroquinone monomethyl ether
M_{nSEC}	number average molecular weight determined by size exclusion chromatography
MW	molecular weight
M_w	weight average molecular weight
MWD	molecular weight distribution
$MW_{micelle}$	molecular weight of a micelle
MW_{mon}	molecular weight of the monomer
MW_{unimer}	molecular weight of a unimer
N_{agg}	aggregation number
NIPAM	N-isopropyl acrylamide
NMP	nitroxide mediated polymerization
PAM	poly(acrylamide)
PAMPS	poly(sodium 2-acrylamido-2-methylpropanesulfonate)

PDI	polydispersity index
PDMA	poly(N,N-dimethylacrylamide)
PDMVBA	poly(N,N-dimethylvinylbenzylamine)
PE	polyelectrolyte
PL	Polymer Laboratories
PNIPAM	poly(N-isopropylacrylamide)
PZ	polyzwitterion
RAFT	reversible addition fragmentation chain transfer
RI	refractive index
R_g	radius of gyration
SEC	size exclusion chromatography
SMFP	smart multifunctional polymer
STPE	sodium 2-(2-thiobenzoylsulfonyl-propionylamino)-ethanesulfonate
USM	University of Southern Mississippi
UV	ultraviolet
VBTAC	*ar*-vinylbenzyltrimethylammonium chloride
λ_w	mobility of water
λ_o	mobility of oil